

12-2009

# Quaternary Deformation Along the Wharekauhau Fault System, North Island, New Zealand: Implications for an Unstable Linkage Between Active Strike-Slip and Thrust Faults

Elizabeth R. Schermer  
liz.schermer@wwu.edu

Timothy A. Little

Uwe Rieser

Follow this and additional works at: [https://cedar.wwu.edu/geology\\_facpubs](https://cedar.wwu.edu/geology_facpubs)

 Part of the [Earth Sciences Commons](#)

---

## Recommended Citation

Schermer, Elizabeth R.; Little, Timothy A.; and Rieser, Uwe, "Quaternary Deformation Along the Wharekauhau Fault System, North Island, New Zealand: Implications for an Unstable Linkage Between Active Strike-Slip and Thrust Faults" (2009). *Geology Faculty Publications*. 7.

[https://cedar.wwu.edu/geology\\_facpubs/7](https://cedar.wwu.edu/geology_facpubs/7)

This Article is brought to you for free and open access by the Geology at Western CEDAR. It has been accepted for inclusion in Geology Faculty Publications by an authorized administrator of Western CEDAR. For more information, please contact [westerncedar@wwu.edu](mailto:westerncedar@wwu.edu).

# Quaternary deformation along the Wharekauhau fault system, North Island, New Zealand: Implications for an unstable linkage between active strike-slip and thrust faults

Elizabeth R. Schermer,<sup>1</sup> Timothy A. Little,<sup>2</sup> and Uwe Rieser<sup>2</sup>

Received 21 November 2008; revised 10 July 2009; accepted 18 August 2009; published 16 December 2009.

[1] The southern Wairarapa region of the North Island of New Zealand preserves a variably deformed late Quaternary stratigraphic sequence that provides insight into the temporal variability in the partitioning of contraction onto faults in the upper plate of an obliquely convergent margin. Detailed mapping, stratigraphic data, and new radiocarbon and optically stimulated luminescence ages from Quaternary units reveal the interaction between tectonics and sedimentation from  $\sim 125$  ka to  $<9$  ka along the Wharekauhau thrust and related faults (i.e., Wharekauhau fault system) at the southern end of the Wairarapa fault zone, a major oblique-slip fault in the upper plate of the Hikurangi Margin. The Wharekauhau thrust accommodated a minimum of  $280 \pm 60$  m of horizontal shortening from  $\sim 70$  to 20 ka. The inferred shortening rate, 3.5–8.4 mm/yr, may have accounted for 11–30% of margin-normal plate motion. By  $\sim 20$  ka, the thrust was abandoned. Subsequent deformation at shallow levels occurred on a segmented fault system that accommodated  $<1$  mm/yr shortening. Active deformation in the region is partitioned between slip on (1) the more western Wairarapa-Mukamuka fault system (dominantly dextral slip but also causing local uplift of the coast); (2) a series of discontinuously expressed strike-slip faults and linking blind oblique-reverse thrusts near the trace of the inactive Wharekauhau thrust; and (3) a blind thrust fault farther to the east. The spatial and temporal complexity of the Wharekauhau fault system and the importance it has had in accommodating upper plate deformation argue for an unsteady linkage between upper plate faults and between these faults and the plate interface.

**Citation:** Schermer, E. R., T. A. Little, and U. Rieser (2009), Quaternary deformation along the Wharekauhau fault system, North Island, New Zealand: Implications for an unstable linkage between active strike-slip and thrust faults, *Tectonics*, 28, TC6008, doi:10.1029/2008TC002426.

<sup>1</sup>Geology Department, Western Washington University, Bellingham, Washington, USA.

<sup>2</sup>School of Geography, Environment and Earth Sciences, Victoria University of Wellington, Wellington, New Zealand.

## 1. Introduction

[2] Oblique convergence along the Pacific-Australia plate boundary in New Zealand has been studied as a natural laboratory for understanding transpression and slip partitioning on fault systems [e.g., Little *et al.*, 2007; Norris and Cooper, 1995; Teyssier *et al.*, 1995; Walcott, 1984]. At oblique subduction zones, plate motion is commonly partitioned between the subduction megathrust and arrays of strike-slip and reverse faults in the upper plate [e.g., Fitch, 1972; McCaffrey, 1992]. In many locations these upper plate faults may pose a greater hazard to society than the megathrust especially where the relatively shallow hypocenters of these earthquakes occur near populated regions. This is the case in Japan (1995 Kobe M7.2), the Cascadia margin of the western U.S. (900AD Seattle fault M  $\sim 7$ ), Nicaragua (1972 Managua M6.2), and New Zealand (1855 Wairarapa M  $\sim 8.2$ ). Although progress has been made understanding how faults in the upper plates of subduction zones accommodate plate motion, there is much we do not yet understand about how these faults interact with each other and with the subduction interface, and how these linkages may change over time. For example, how similar is the pattern by which upper plate faults and fault segments interact with one another on short (e.g.,  $10^2$ – $10^3$  years, seismic cycle) versus on long ( $10^4$ – $10^6$  years) time scales? What factors determine the stability of fault segments and how is this recorded in the landscape? How is strain partitioned among oblique, reverse, and strike-slip faults and between the hanging wall and subduction zone faults on different timescales?

[3] Active faults in the upper plate of the Hikurangi margin of New Zealand form a complex array of strike-slip, oblique-slip, and reverse faults (Figure 1). Most of New Zealand's largest historical earthquakes have occurred on these faults, including in 1855 (M  $\sim 8.2$ ), 1931 (M7.8), and 1934 (M7.6). The Wairarapa fault zone (Figures 1 and 2), one of the major fault zones in the North Island, plays an important role in accommodating upper plate deformation [e.g., Beanland and Haines, 1998; Wallace *et al.*, 2004]. The 1855 Wairarapa earthquake, which produced surface rupture along the Wairarapa fault zone (Figure 1) [Grapes and Wellman, 1988; Grapes and Downes, 1997; Lyell, 1856; Ongley, 1943], resulted in up to 6.4 m of coastal uplift, and up to  $\sim 18.5$  m of dextral slip, the largest coseismic rupture documented for an historical earthquake worldwide [McSaveney *et al.*, 2006; Rodgers and Little, 2006]. Despite the proximity of the southern part of the Wairarapa fault zone to New Zealand's capital city of Wellington and

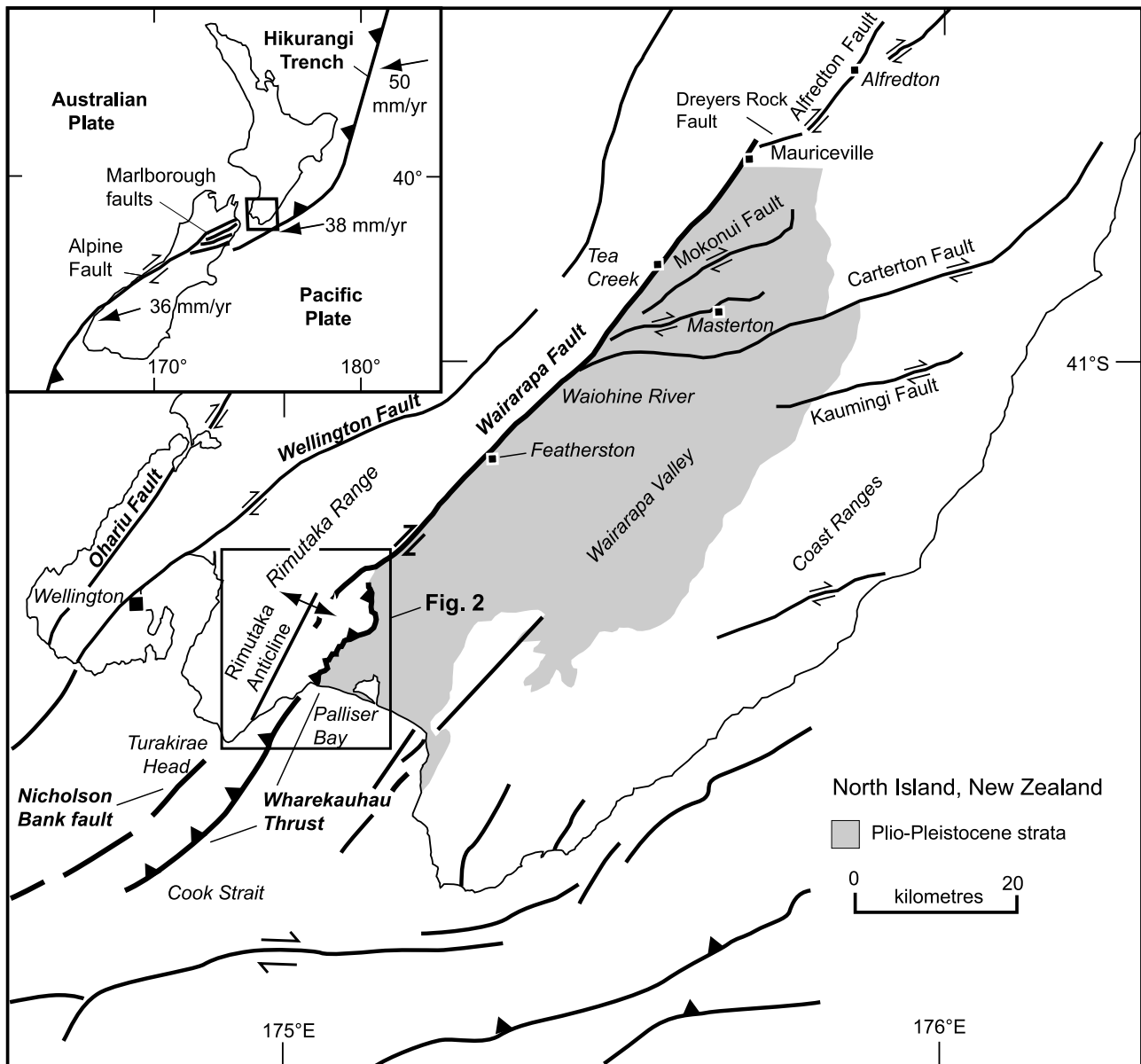


**Figure 1.** Generalized map showing major active faults and other structures of the southern North Island, New Zealand [after Barnes, 2005; Begg and Johnston, 2000; Lee and Begg, 2002], localities mentioned in text and box outlining Figure 2. Inset shows plate tectonic setting of New Zealand (plate motions taken from DeMets *et al.* [1990, 1994]).

the seismic hazard that it poses, there are surprisingly few constraints on the structural geology of the fault, the geometry and location of its earthquake ruptures, or on the relationship of Wairarapa fault earthquakes to uplifting of the Rimutaka Range and the coastal platform. Preserving a rich and variably deformed late Quaternary stratigraphic sequence, and benefiting from several superb coastal exposures, the region is also of special interest for the insight it can provide on the temporal variability (since  $\sim 125$  ka) in the partitioning of contractional fault slip onto (and off) a major fault on the upper plate of an obliquely convergent subduction zone.

[4] In this paper we present stratigraphic, geomorphic, and structural data to document Quaternary deformation along the Wharekauhau thrust and related faults (Wharekauhau fault system) at the southern end of the greater Wairarapa fault zone (Figure 2). Our aim is to understand the structural development of the Wharekauhau fault system and the style of its rupture (if any) during the 1855 and earlier earthquakes, and to constrain the short- and long-term slip rates on this part of the Wairarapa fault zone. We document major spatial and temporal changes in strain partitioning at the southern end of the greater Wairarapa fault zone, including a brief ( $\sim 50$  ka) period of rapid slip on the Wharekauhau

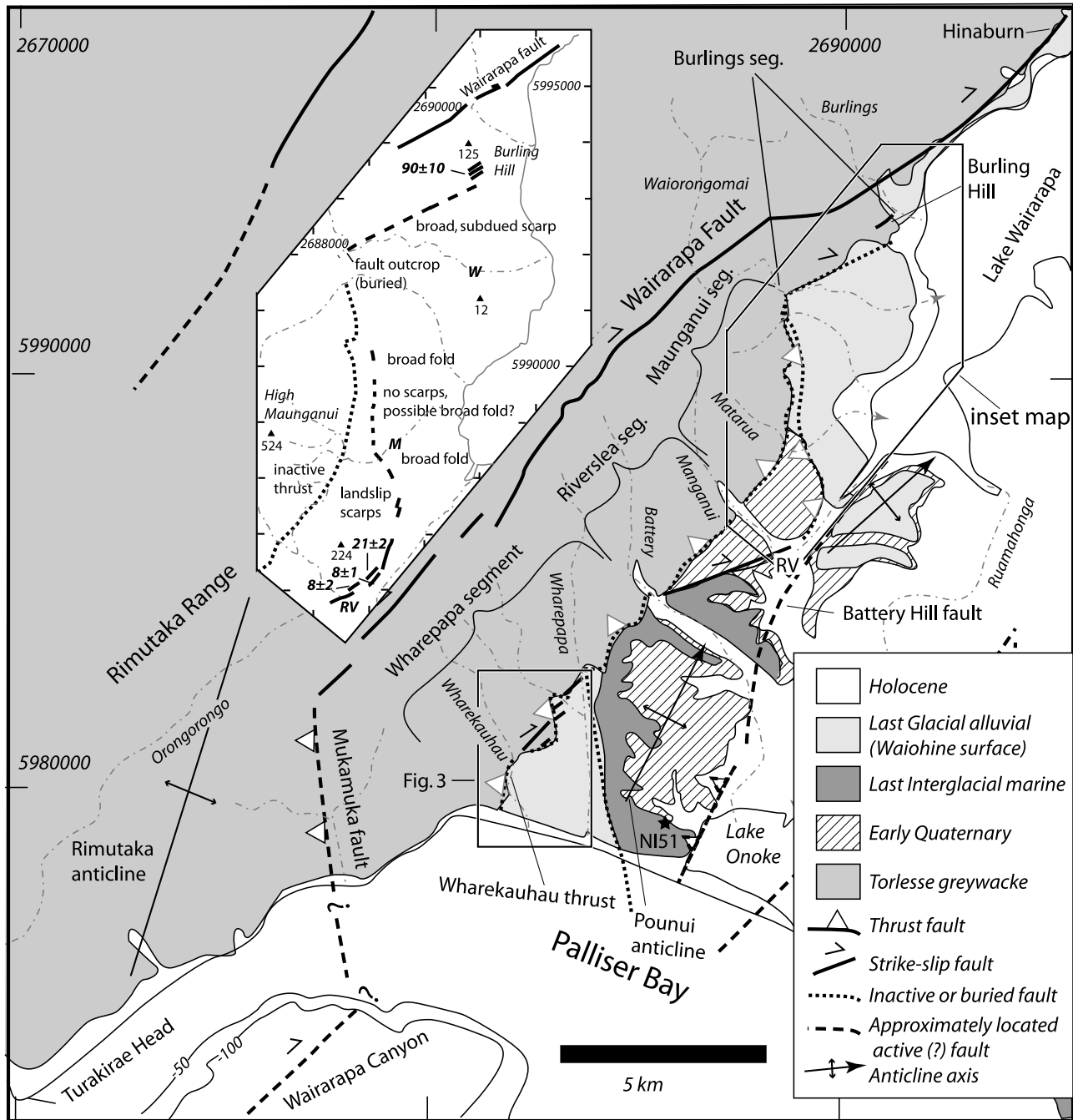


**Figure 2.** Quaternary to Recent fault traces and folds along the Wharekauhau fault system in the southern part of the Wairarapa fault zone. Geologic map base simplified from *Begg and Johnston* [2000], revisions by *Little et al.* [2008]. Segments of Wharekauhau thrust are discussed in text; stream names are shown in italics. Boxes outline inset to left and location of Figure 3. Star indicates location of OSL sample NI51. Inset shows enlarged map of Maunganui segment and part of Riverslea segment. Bold numbers indicate locations where dextral separation of surface features was measured in this study. W, Wairongomai River; M, Matarua Stream; RV, Riverslea. Grid marks (in meters) refer to the New Zealand Map Grid Coordinate System.

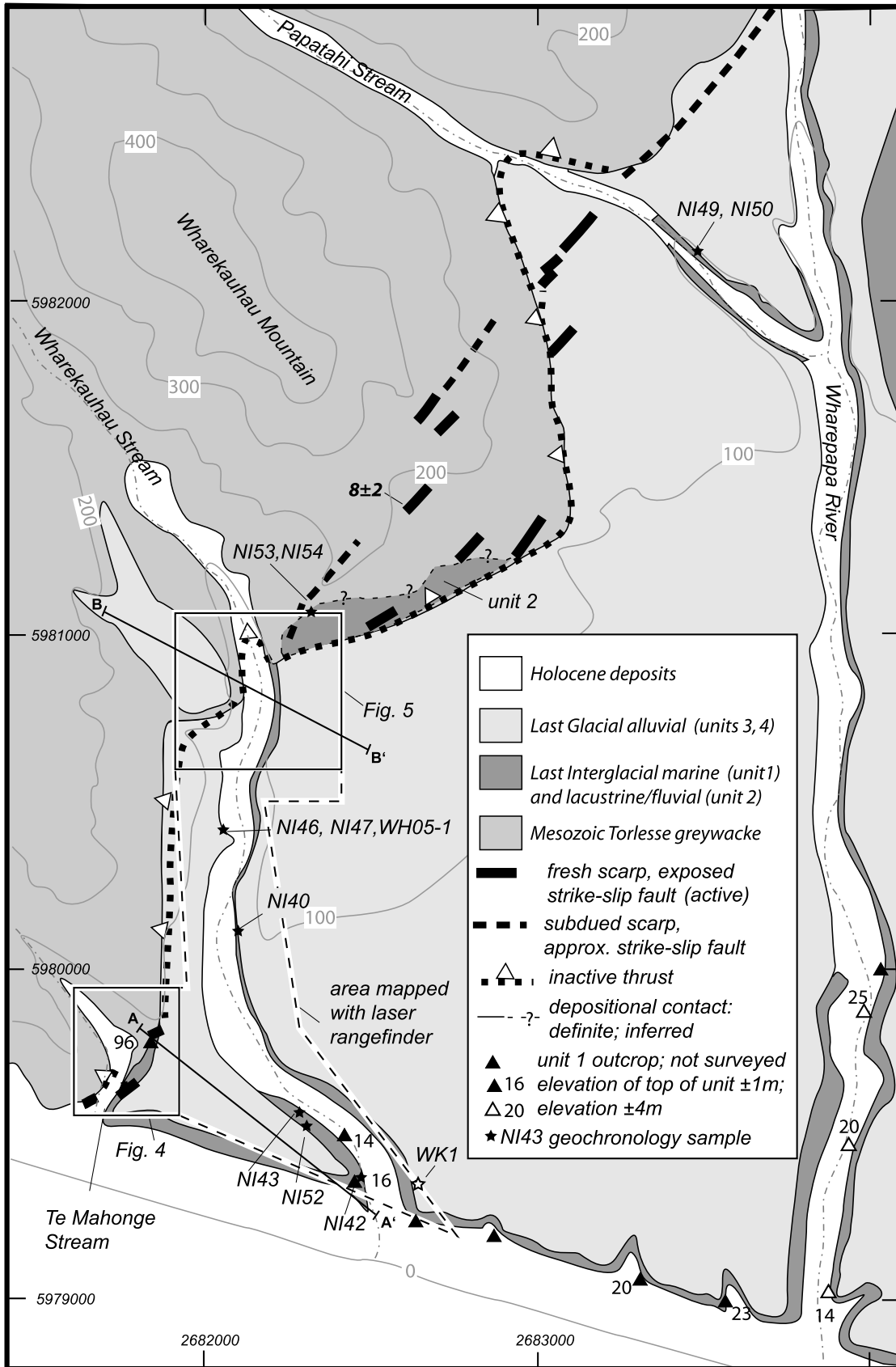


Figure 3

thrust. We analyze the implications of these data for the kinematic linkage between the Wairarapa, Wharekauhau, and adjacent faults at different times.

## 2. Tectonic Setting

[5] The Pacific-Australia plate boundary in the North Island of New Zealand accommodates oblique subduction of oceanic crust along the Hikurangi margin of the North Island, and oblique continental collision in the South Island (Figure 1). In the southernmost North Island, the contemporary oblique plate convergence of  $\sim 42$  mm/yr can be broken down into  $\sim 30$  mm/yr of margin-orthogonal motion and  $\sim 28$  mm/yr of margin-parallel motion [Beavan *et al.*, 2002]. The convergent component is accommodated by thrust faults and related folds in the offshore region and adjacent to the southeast coast, and by contractional slip on the subduction megathrust beneath these faults, which is thought to be strongly “coupled” in the southern part of the North Island [Barnes and Mercier de Lépinay, 1997; Barnes *et al.*, 1998; Nicol *et al.*, 2002, 2007; Nicol and Wallace, 2007]. The margin-parallel component is accommodated by strike slip and dextral-reverse slip on the North Island Dextral fault belt (NIDFB), an array of NNE striking faults, including the Wellington and Wairarapa faults (Figure 1) [e.g., Beanland, 1995; Mouslopoulou *et al.*, 2007; Van Dissen and Berryman, 1996], by clockwise vertical axis rotation of an eastern part of the North Island [Nicol *et al.*, 2007; Wallace *et al.*, 2004], by strike slip on active ENE striking structures in Cook Strait, and by oblique slip on other, NE striking offshore faults, including the subduction megathrust [Barnes and Mercier de Lépinay, 1997; Barnes *et al.*, 1998; Barnes and Audru, 1999]. Seismicity data suggest that faults of the NIDFB intersect the subduction zone at depths of 20–30 km beneath the Wairarapa region [Reyners, 1998]. GPS geodetic data suggest that this segment of the subduction interface is currently “locked” and is accumulating elastic strain [Wallace *et al.*, 2004]. The interaction of the subducting plate interface and faults of the NIDFB is poorly understood, although GPS modeling suggests that the locked megathrust is loading at least some of the crustal faults at depth beneath the southern North Island [Darby and Beaven, 2001; Wallace *et al.*, 2004]. Rodgers and Little [2006] have suggested that the 1855 earthquake coruptured the Wairarapa fault and a part of the subduction interface.

### 2.1. Geology of the Wairarapa Fault Zone

[6] The Wairarapa fault is interpreted to have been initiated in the Pliocene as a reverse fault and reactivated as a strike slip fault at  $\sim 1$ – $2$  Ma in response to a clockwise

vertical axis rotation of the fore arc relative to the Pacific Plate [Beanland, 1995; Beanland and Haines, 1998; Kelsey *et al.*, 1995]. The dextral-reverse fault, dipping steeply northwest, extends from Mauriceville in the north to Lake Wairarapa in the south (Figures 1 and 2). In the southern Wairarapa, the Wairarapa fault is the easternmost strike-slip fault in the NIDFB, while margin-perpendicular shortening is accommodated by folding and thrusting further to the east [Formento-Trigilio *et al.*, 2003; Nicol *et al.*, 2002]. The northern and central sections of the Wairarapa fault are typically expressed by a  $\sim 250$ – $500$  m wide zone of mostly left-stepping en echelon traces [Grapes and Wellman, 1988; Rodgers and Little, 2006]. Southwest of Lake Wairarapa, the fault trace is more complex: a western strand continues southwestward into the Rimutaka Range, whereas an eastern strand steps eastward  $\sim 5$ – $6$  km before deflecting back to a southwestward trend and bordering the range front as far as the southern coast [Begg and Mazengarb, 1996; Begg and Johnston, 2000; Grapes and Wellman, 1988] (Figure 2).

### 2.2. Wharekauhau Fault System

[7] We refer to the faults that comprise the eastern strand of the greater (southernmost) Wairarapa fault zone as the “Wharekauhau fault system.” This strand has been previously interpreted to consist of an active thrust fault termed the Wharekauhau thrust that is also inferred to have been a locus of surface rupturing during the 1855 earthquake [Begg and Mazengarb, 1996; Begg and Johnston, 2000; Grapes and Wellman, 1988]. For this paper, we will restrict the term “Wharekauhau thrust” to a specific thrust that is well exposed near the Palliser Bay coast and emplaces Mesozoic greywacke in its hanging wall over Quaternary strata in its footwall. As we document below, we infer this major fault to be inactive and not to have ruptured (at least as a thrust) in 1855. Other smaller-displacement (and in part younger and steeper dipping) faults in Wharekauhau fault system are clearly active dextral-slip (or dextral-reverse) structures, some of which did rupture in 1855, but we do not refer to these as the “Wharekauhau thrust.”

[8] The Wharekauhau thrust separates uplifted Mesozoic greywacke on the northwest from Quaternary strata of the Wairarapa basin on the southeast. Quaternary strata in the footwall of the fault consist of last interglacial marine deposits and alluvial fan gravels derived from the Rimutaka Range. The most widespread and conspicuous of these are the latest Pleistocene to Holocene fan gravels referred to as the “Waiohine gravels” by many previous workers in the region (Figures 2 and 3). The top surface of this abandoned fan (the “Waiohine surface”) has been widely mapped along the western side of the Wairarapa valley and dips gently eastward beneath Lake Wairarapa [Begg and Johnston, 2000;

**Figure 3.** Geology of Wharekauhau segment, showing Quaternary unit designations as described in text, fault and fold traces, and sample locations (not including samples shown in Figures 4 and 5). Open star shows sample location from Wang [2001]. Outcrops of unit 1 are indicated by filled triangles; where surveyed, the elevation of the top of unit 1 is indicated. No outcrops of unit 1 occur north of the northernmost symbols. Open triangles indicate locations with elevations estimated from topographic maps. Dashed outline shows area of detailed mapping and laser surveying, two portions of which are detailed in Figures 4 and 5. Location of cross sections A-A' and B-B' (Figures 4b and 5b) are indicated. Topographic contours are in meters; grid marks (in meters) refer to the New Zealand Map Grid Coordinate System.

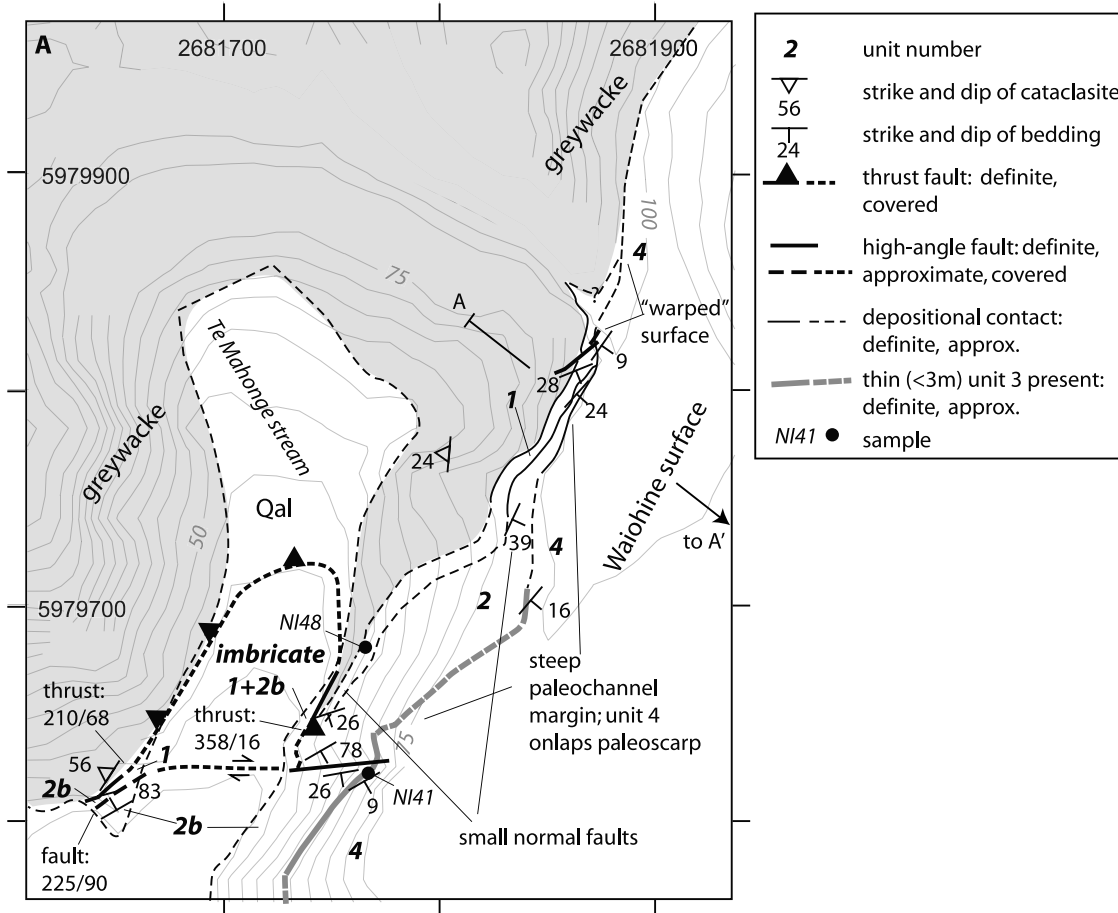


**Figure 4a.** Detailed map of Te Mahonge stream area derived from surveying topography and geologic contacts with a laser rangefinder. We used ~3500 surveyed points to generate a 1:2500 scale map with a 2 m contour interval, but for clarity we present the results with a 5 m contour interval. All Quaternary units are left unpatterned for clarity. Locations of geochronological samples are shown with black dots. West end of cross section line A-A' is shown.

Lee and Begg, 2002]. New <sup>14</sup>C data constraining the age of the Waiohine surface at 12–10 ka [Little et al., 2009], combined with dextral offsets of 99–130 m across the active trace of the Wairarapa fault [Grapes and Wellman, 1988; Lensen and Vella, 1971; Little et al., 2009], suggest a Late Quaternary dextral slip rate for the Wairarapa fault of 8–15 mm/yr [Grapes and Wellman, 1988; Lensen and Vella, 1971; Little et al., 2009; Van Dissen and Berryman, 1996; Wang, 2001]. Slip rates have never been measured for any faults in the Wharekauhau fault system.

[9] For this study we mapped the Wharekauhau fault system from its northern intersection with the Wairarapa fault to the Palliser Bay coast (Figure 2). We mapped and analyzed faults, measured offset landscape features, and looked for evidence of 1855 surface rupture. Where the thrust is best exposed near the coast, we surveyed the position of faults and stratigraphic contacts with a laser range finder (MDL LaserAce 300 with horizontal angle encoder). These surveys were tied to control points established by GPS, and were used to generate a set of quantitative and detailed geologic maps (Figures 3, 4, and 5).

Combined errors, due to instrument error that increases with distance and our inability to accurately locate some contacts in bush, are estimated from repeated surveys of the same contact to be ±1 m in both the vertical and horizontal for shot lengths up to 120 m. We also examined the stratigraphy of faulted and unfaulted units, and obtained four new radiocarbon and eleven new optically stimulated luminescence (OSL) ages from Quaternary units in this detailed study area. After describing the stratigraphic context of the Wharekauhau thrust, we focus on structural and geomorphic observations and interpretations of the Wharekauhau fault system, from north to south. We then discuss the implications of temporal and spatial variations in deformation during late Quaternary time.

### 3. Stratigraphic Framework of the Southern Wairarapa Fault Zone and Wharekauhau Thrust

[10] Near the south coast of the Wairarapa Valley, late Quaternary strata and their corresponding landforms, such

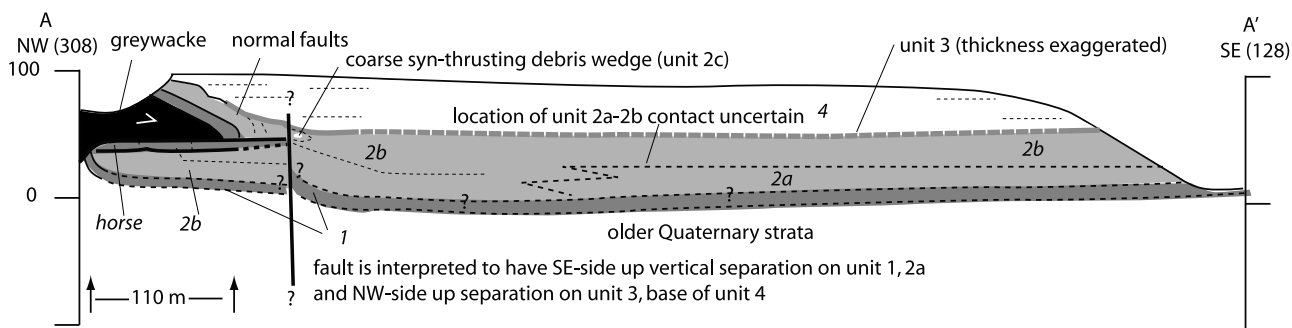


**Figure 4b.** Cross section A-A', no vertical exaggeration, constructed perpendicular to the average cataclastic strike of 218 (N38E). Location is shown on Figure 3. Fine dashed lines show bedding traces. For details within the horse, see Figure S1.

as wave-cut platforms and fluvial terrace surfaces, record a progression of relative sea level changes, periods of deposition, and pulses of deformation near the Wairarapa fault since ~125 ka. To the west of the Wharekauhau thrust, late Quaternary strata were deposited unconformably above Mesozoic greywacke, whereas to the east of the thrust, the same strata overlie a substrate of Pliocene-Pleistocene marine to nonmarine strata [e.g., *Begg and Johnston, 2000*]. The late Quaternary sequence provides a sensitive geological record of landscape evolution and deformation (folding and fault slip). In this section we summarize previous work and present new stratigraphic and geochronologic data relating to the Quaternary deposits, with special focus on the areas of Te Mahonge and Wharekauhau streams (Figures 3, 4, and 5 and Text S1 and S2 in the auxiliary material).<sup>1</sup> Unit designations used here are newly defined and do not necessarily correspond to (varied) nomenclature used in the earlier work (most of which is unpublished); detailed unit descriptions and a comparison of nomenclature are provided in Text S1.

### 3.1. Quaternary Stratigraphy and Geochronology of the Wharekauhau Region

[11] The oldest exposed part of the sequence consists of fluvial sands, silts and gravels of early to middle Quaternary age (Te Muna and Ahiaruhe formations [*Begg and Mazengarb, 1996; Collen and Vella, 1984*]). In the area west of Lake Onoke, *Ghani* [1978] inferred that the Te Muna formation is inset by at least four wave-cut terraces of inferred last interglacial age that are overlain by marginal marine sands and gravels. To the east of Wharepapa River, these terraces range in height from 40 to 160 m asl [*Begg and Mazengarb, 1996*] (Figure 2). Farther to the west, the terraces are buried beneath younger deposits. Our studies focused on the marine, lacustrine, and fluvial strata overlying the terraces. Detailed mapping and surveying of these younger strata suggest that most of the units undergo lateral facies and thickness changes, reflecting a tectonic or geomorphic influence of the adjacent Wharekauhau thrust.

<sup>1</sup>Auxiliary materials are available in the HTML. doi:10.1029/2008TC002426.

[12] Local exposures of marine sands and gravels west of Wharepapa River, herein termed unit 1, occur as a 7–9 m thick sequence in the hanging wall and footwall of the Wharekauhau thrust. As the base of unit 1 is only exposed locally, and its top is typically buried by younger strata in areas >300 m north of the coast (Figure 3), we could not document facies or thickness variations in this unit. In the hanging wall, unit 1 overlies greywacke bedrock, while in the footwall, unit 1 overlies fluvial gravels possibly belonging to the Te Muna Formation (Figures 4 and 6) [*Eade, 1995; Grapes and Wellman, 1993; Marra, 2003*].

[13] In the footwall of the Wharekauhau thrust, the marine gravels are overlain conformably by ~9 m of organic-rich lacustrine mud, silt, and gravelly silt that locally contains tree stumps in growth position (unit 2a). This unit is interpreted to have been deposited during an interglacial climate in an estuarine lagoon similar to present-day Lake Onoke [*Eade, 1995; Marra, 2003; Shulmeister et al., 2000*]. Unit 2a interfingers northward and westward with, grades laterally into, and is overlain by fluvial gravels containing clasts eroded from the Rimutaka Range (unit 2b). Unit 2b locally includes intercalations of organic-rich muds up to 1 m thick. Toward the top of unit 2b, gravels have a distinctive yellowish brown color and contain local thin (<0.5 m) silt beds with rooted stumps in growth position. These poorly sorted yellowish brown gravels are widespread, up to 20 m thick, and locally overlie other, more well-sorted gravels of unit 2b and silts of unit 2a along an irregular erosion surface [*Eade, 1995*].

[14] Unit 2 coarsens and thickens toward the trace of the Wharekauhau thrust, where the silts and muds of unit 2a are replaced to the north and west by the angular gravels of unit 2b, and where we recognize a locally exposed bouldery facies, unit 2c (Figures 6, 7, and 8 and Text S1). Only found adjacent to the thrust, unit 2c consists of massive, coarse, very poorly sorted silty gravels that are 1–3 m thick. (Figures 8 and S2). For mapping purposes we have combined units 2a, 2b, and 2c because only unit 2b is widely exposed. Because of the small scale of interfingering and the abrupt facies changes, we lump units 2a, 2b, and 2c together to calculate the thickness of unit 2, but the values are dominated by the thickness of unit 2b (Figure 7).

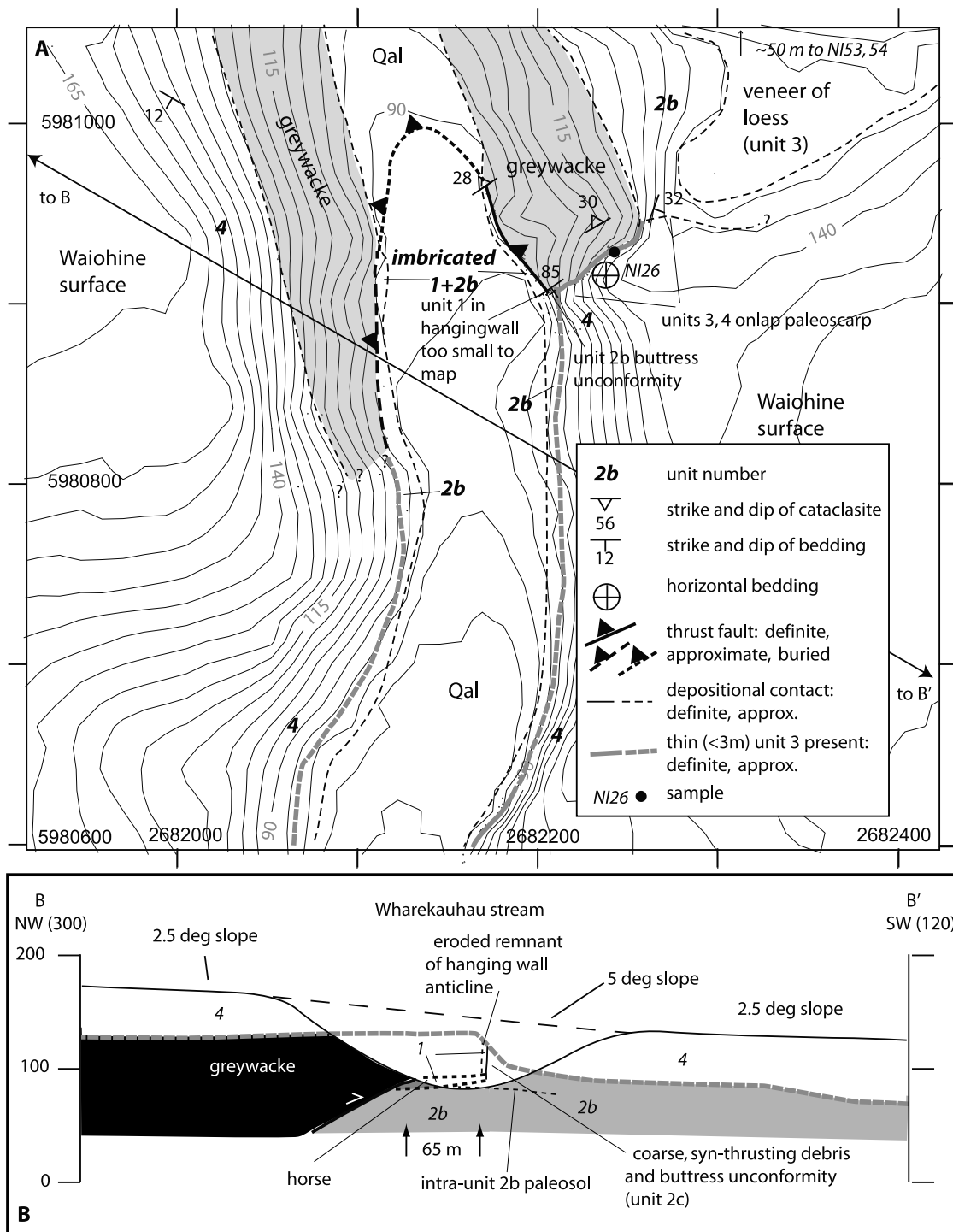


**Figure 5.** (a) Detailed map of Wharekauhau stream area derived from surveying topography and geologic contacts with a laser rangefinder. We used ~4000 surveyed points to generate a 1:2500 scale map with a 2 m contour interval, but for clarity we present the results with a 5 m contour interval. Locations of geochronological are shown with black dots. East end of cross section line B-B'' is shown. (b) Cross section B-B', no vertical exaggeration constructed perpendicular to a thrust strike of 210 (N30E) consistent with the structure contours drawn across Wharekauhau stream and the regional trend of the fault. Location is shown on Figure 3. Fine dashed lines show bedding traces.

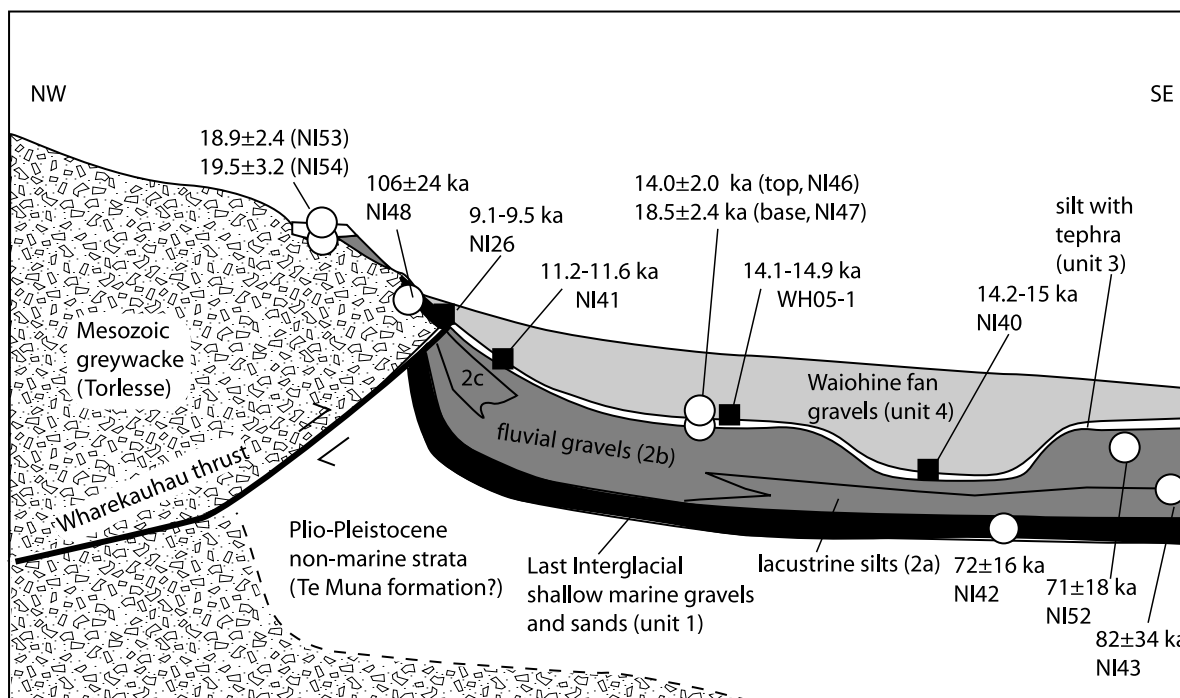


**Figure 6.** Schematic cross section of stratigraphy in the detailed study area of Figure 3. Squares indicate locations of radiocarbon samples (wood from in situ roots, stumps); circles indicate locations of OSL samples (silts, fine sands). Age ranges for radiocarbon samples are calibrated age range at 95% confidence. Errors on OSL ages are  $2\sigma$ . See Figures 2, 3, 4, and 5 for detailed sample locations and Tables 1a, 1b, and 2 for geochronologic data.

[15] Strata in the upper part of unit 2 record evidence of tectonic activity. Upper and lower parts of unit 2b are separated by a soft, red-brown gravelly clay that we interpret as a paleosol (Figure 8 and Text S1). Unit 2c is only found above this clay, and the coarse gravels interfinger southeastward with better sorted and stratified gravels typical of the upper part of unit 2b. Unit 2c occurs in fault contact beneath a lower imbricate of the Wharekauhau thrust, and also in discordant depositional contact against steeply dipping strata of unit 1 in the hanging wall of the thrust (Figure 8). We interpret this discordant contact as a buttress unconformity and unit 2c to represent colluvium derived from the thrust scarp. Older parts of the unit were overthrust during fault slip, while younger parts were deposited against the emergent hanging wall, partially burying it. Unit 2 thickens from 11.5 to  $>46$  m westward in the footwall of the Wharekauhau thrust (italic thickness values in Figure 7), but isopachs of unit 2 thickness were not constructed because neither the top nor bottom of the sequence is exposed over sufficient area. We interpret the thickening to reflect proximity to the topographic scarp of the Wharekauhau thrust, an inference that is strongly supported by the syntectonic facies relationships shown in Figure 8, and the replacement of unit 2a by unit 2b toward the thrust (Figures 4 and 6). An alternative explanation, that the thickness and facies changes are related to the (non-tectonically controlled) geometry of the lagoon and alluvial fan environments, seems less likely as the thickest sections

of unit 2 appear to be unrelated to the major, modern streams (e.g., Wharepapa River; Figure 7).

[16] Unit 3, a widespread sandy silt averaging  $\sim 2$  m thick, caps the unit 2b gravels. *Grapes and Wellman* [1993] reported that this silt contains shards of the Kawakawa tephra (26,500 calibrated (calib) years B.P. [*Wilson et al.*, 1988]) and abundant in situ stumps and roots at its top dated at  $12,450 \pm 120$  and  $12,760 \pm 110$   $^{14}\text{C}$  years B.P. [*Grapes and Wellman*, 1993] (these correspond to calibrated ages of  $\sim 15$  ka). *Grapes and Wellman* [1993] interpreted the silt as a loess deposited on an abandoned fan surface, but the local presence of poorly sorted fine pebbles in the unit led *Shulmeister et al.* [2000] to reinterpret the unit as an over-bank deposit mixed with loess. Unit 3 is overlain by alluvial fan gravels (“Waiohine gravels,” unit 4) that are topped by the terrace tread referred to as the Waiohine surface by *Grapes and Wellman* [1993]. *Wang* [2001] reported a  $\sim 5$  ka OSL age on a silt lens collected 0.6 m beneath this surface at Wharekauhau Stream (sample WK-1; Figure 3).

[17] Our work shows that units 3 and 4 overlap the Wharekauhau thrust and units 1 and 2 along a marked angular unconformity. In the footwall of the thrust, unit 3 typically occurs as a 1–2 m thick layer above unit 2 (Figure 6). In the hanging wall, unit 3 varies in thickness from  $<0.5$  to  $\sim 6$  m, overlies Mesozoic greywacke and unit 2 (Figures 5 and 8), and locally is omitted beneath the erosional base of unit 4 (Figure 4). Thickness variations and the massive nature of the silt in the hanging wall

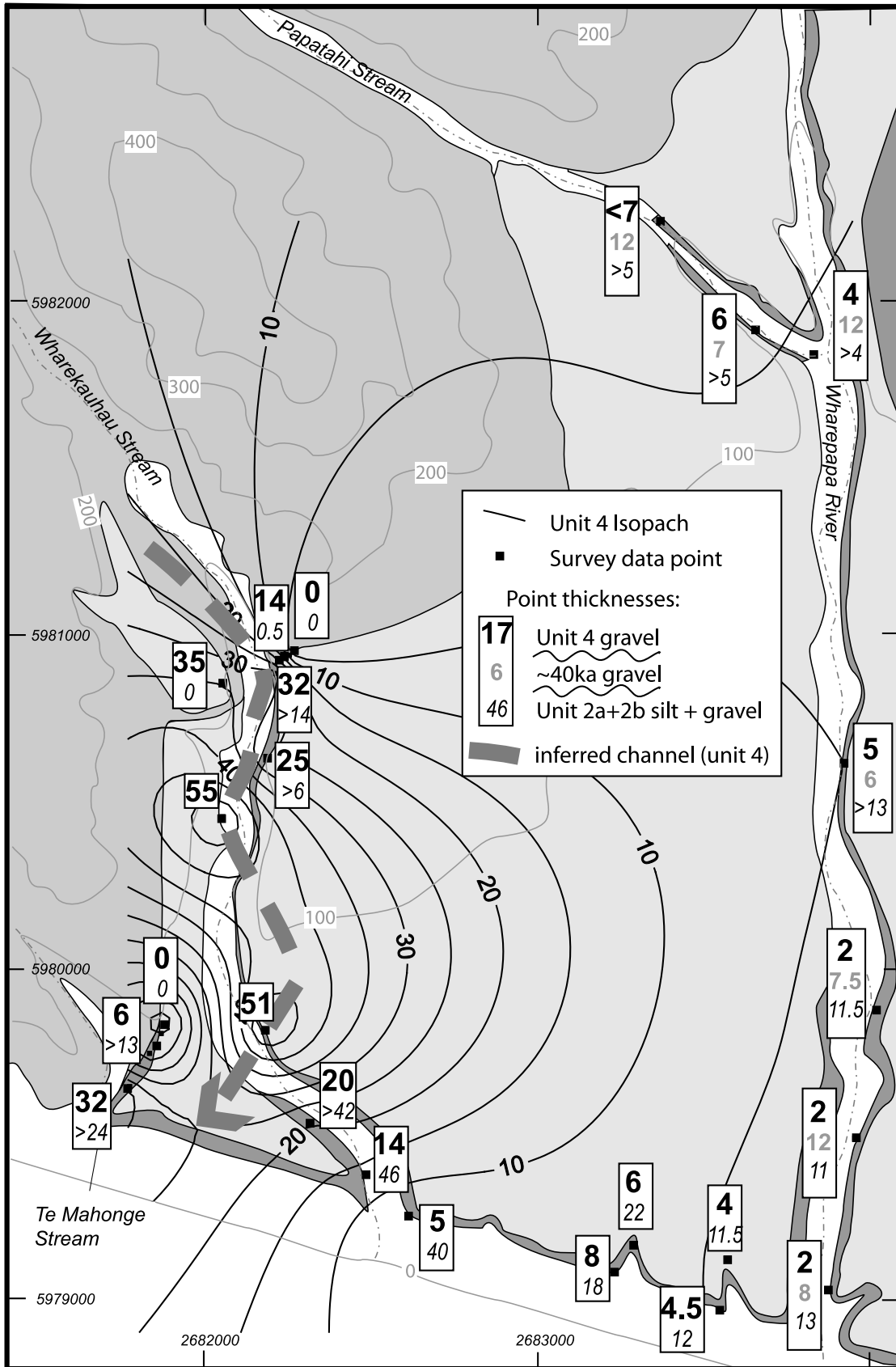


Figure 7

suggest that the fault-proximal part of unit 3 is a loess that mantles a paleoscarp formed in older units (Figures 5 and 8 and Text S1). The angular discordance between unit 3 and older Quaternary strata is typically  $\sim 15^\circ$ , but locally up to  $\sim 80^\circ$  (Figures 4, 5, and 9a). The discordance disappears to the southeast away from the thrust (Figure 4b).

[18] In contrast to unit 2, there are no obvious facies changes in units 3 and 4 toward the Wharekauhau thrust, and both units thin in that direction, implying an onlapping relationship (Figures 6 and 7). Adjacent to the thrust, the deformed and eroded surface of unit 2 and older units forms a NNE trending paleoscarp against which the unit 4 gravels, up to 50 m thick in the southeast, pinch out toward the northwest (Figures 4, 5, and 8). At Te Mahonge Stream the pinchout coincides with a very steep north to northeast trending paleochannel wall (exposed in outcrop) that cuts  $>8$  m downward into units 2 and 3 (Figure 4). The thickest unit 4 gravels occur to the east of this paleochannel wall. Isopachs of unit 4 appear to cross the trace of the thrust, however only one thickness measurement was obtained northwest of the thrust trace (Figure 7).

[19] The map pattern and thickness variations indicate that deposition of units 3 and 4 was strongly influenced by an earlier scarp generated along the Wharekauhau thrust. The angular unconformity beneath these two units, their overlapping of the thrust, and their subhorizontal attitude indicates the thrust was not active at the time of deposition (or subsequently). The lithologic characteristics and isopachs of unit 4 suggest that it was deposited as a small, steep, and locally sourced fan that was derived from the hanging wall to the west (Figure 7 and Text S1).

### 3.2. OSL and $^{14}\text{C}$ Dating

#### 3.2.1. Methods

[20] We sampled fine sands and silts from each unit for optically stimulated luminescence (OSL) dating at Victoria University, Wellington (Tables 1a and 1b). The OSL dating approach was multiple aliquot additive dose IRSL on the polymineral 4–11  $\mu\text{m}$  fraction [Lang and Wagner, 1997], which selectively stimulates feldspars by 880 nm infrared light. The Riso TL-DA15 luminescence reader was equipped with optical filters Kopp 5–58 and Schott BG39 to ensure the exclusive measurement of the 410 nm feldspar emission band, which is known to minimize fading effects. Anomalous fading was insignificant, as proved by a standard test after 6 months storage. The dose rate was obtained from a gamma spectrometry measurement using an ultra-low background Canberra BE-50 germanium detector. The activity concentrations of  $^{40}\text{K}$ ,  $^{208}\text{Tl}$ ,  $^{212}\text{Pb}$ ,  $^{228}\text{Ac}$ ,  $^{214}\text{Bi}$ ,  $^{214}\text{Pb}$  and  $^{226}\text{Ra}$  form the basis of the dose rate calculation

using the conversion factors by Adamiec and Aitken [1998]. The cosmic dose rate calculation follows Prescott and Hutton [1994].

[21] We also obtained samples of wood for radiocarbon dating. Radiocarbon samples were dated at Waikato University, with results and methods listed in Table 2.

#### 3.2.2. Results

[22] The schematic structural and stratigraphic position of each sample are shown in Figure 6. OSL dates discussed in this section are quoted with  $2\sigma$  errors (i.e., twice the lab-reported error in Tables 1a and 1b), and  $^{14}\text{C}$  ages are quoted as calibrated age ranges at the  $2\sigma$  confidence interval.

[23] Three samples collected from widely spaced outcrops of the last interglacial shallow marine sands yielded somewhat variable OSL ages (Tables 1a and 1b and Figure 6) that are indicative of the last interglacial sea level highstand (oxygen isotope stage (OIS) 5). The oldest sample (NI51), from a  $>4$  m thick unit of well-sorted sands and gravels at  $\sim 40$  m elevation east of Wharepapa River (Figure 2) is interpreted as a last interglacial beach deposit. It is overlain by  $\sim 25$  m of inferred fluvial deposits of unknown age that underlie an extensive terrace surface. Neither the beach deposit nor the overlying fluvial strata are in stratigraphic continuity with the fault-proximal units 1 and 2 described above, so we have not attempted to correlate them. This sample yielded an age of  $127 \pm 20$  ka, consistent with this deposit having mantled a wave cut platform that formed during OIS 5e. Sample NI48 was collected from deformed unit 1 in the hanging wall of the thrust in Te Mahonge Stream at 46 m elevation (Figure 4). This sample yielded an age of  $106 \pm 24$  ka, within error of NI51, and also suggests a last interglacial age (though not necessarily stage 5e). An undeformed (flat-lying) sample of unit 1 (NI42) collected from the footwall of the thrust at 13 m elevation (Figure 3) yielded an age of  $71 \pm 8$  ka, consistent with OIS 5a. The different locations, structural settings, and the higher elevation and older age of sample NI51 relative to NI42 (Figures 2 and 3) suggest their deposition during different sea level highstands (substages) within OIS 5. Given the analytical errors, we cannot distinguish whether the two samples of unit 1 (NI48 and NI42) were deposited during different substages or during OIS5a.

[24] Samples from unit 2 yielded OSL ages that are consistent with deposition near the end of the last interglacial at  $\sim 80$ – $70$  ka (i.e., OIS 5a). Sample NI43 from the lower part of unit 2b yielded an age of  $82 \pm 34$  ka (Figures 3 and 6). This sample is located  $\sim 4$  m above silts of unit 2b dated by OSL at  $\sim 115 \pm 66$  ka [Marra, 2003] and  $\sim 16$  m above a sample of unit 2a dated at  $117 \pm 60$  ka [Marra, 2003] ( $2\sigma$  errors). A higher sample from unit 2b,  $\sim 20$  m above sample NI43, yielded an age of  $72 \pm 16$  ka (sample

**Figure 7.** Map showing isopachs of thickness of unit 4, with inferred paleochannel location indicated by gray dashed line along thickest deposits. Isopachs are superimposed on geologic units and fault traces from Figure 3. Data point values indicate thickness of unit 4 (upper bold number), thickness of unit 2 (lower italic number). Where three values are shown, the middle value indicated in gray is the inferred thickness of  $\sim 40$  ka gravels dated at locality NI49; these gravels are correlated along Wharepapa River via their location above a prominent paleosol but have not been dated except in Papatahi Stream. Thicknesses are calculated from maps in Figures 3, 4, and 5 and at spot locations along coastal and stream bluffs by shooting the top and bottom contacts with a laser rangefinder.

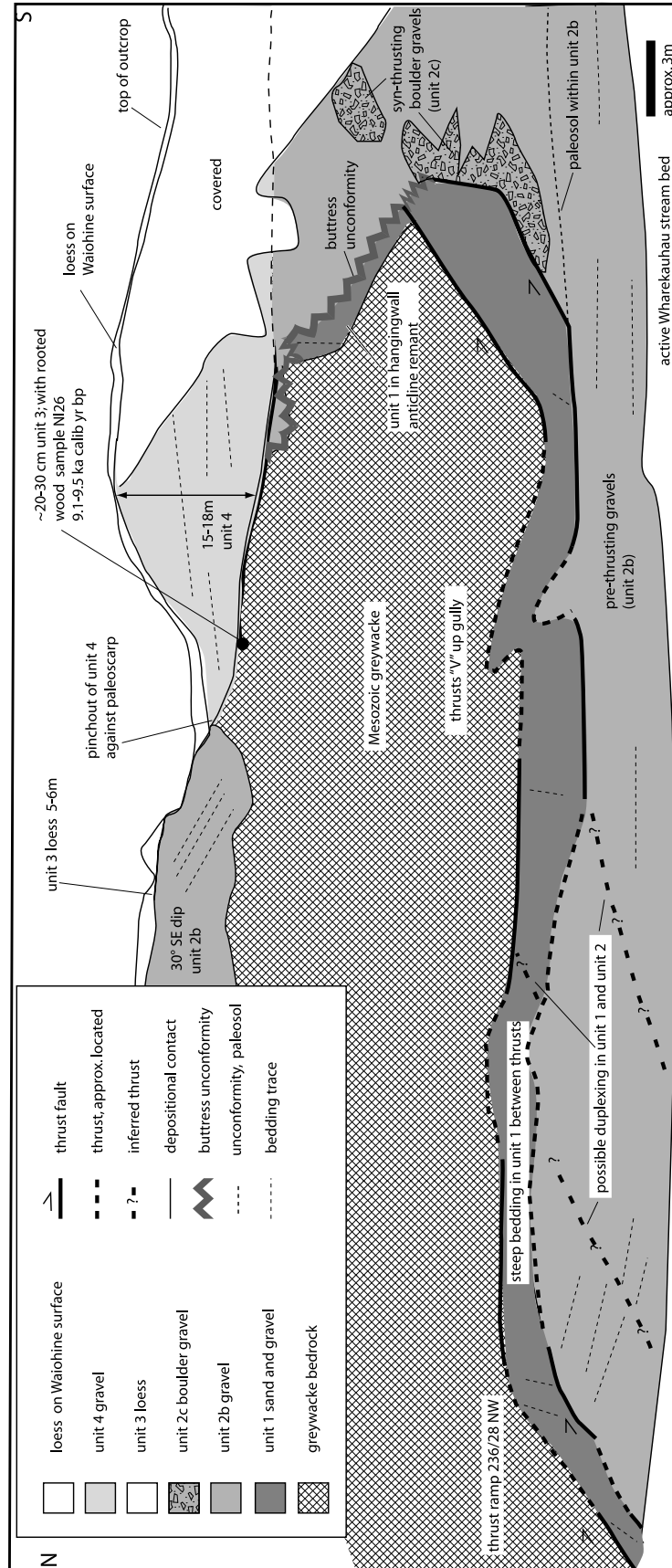


**Figure 8.** Tracing of a photomosaic of an outcrop of the thrust on the east bank of Wharekauhau stream (NE corner of Figure 5). Duplexing in unit 2b is inferred from discontinuities in bedding; duplexing in unit 1 is inferred from extreme thickening of unit 1 in horse relative to undeformed exposures. Photomosaic is shown in Figure S2.

NI52, Figures 3 and 6). We note that our dating accords with the last interglacial interpretation of these units by *Grapes and Wellman* [1993] and *Shulmeister et al.* [2000] and the interpretations of *Marra* [2003] based on the fossil insect assemblage in unit 2a. The highest unit 2 sample

(NI52) is from  $\sim 10$  m below the paleosol (unit 3) that marks the abandonment of this fan surface and thus is close to the end of this phase of gravel aggradation.

[25] All the unit 2 samples from this study are within  $2\sigma$  error of the youngest unit 1 sample (NI42,  $71 \pm 8$  ka). However, the samples of *Marra* [2003] are stratigraphically above NI42 and do not overlap that age within  $2\sigma$  error, suggesting either the latter age is too young or *Marra's* unit 2 ages are too old. We note that the unit 2 samples typically contain very high radionuclide contents (Tables 1a and 1b), causing saturation of the OSL signal and thus reducing the datable age range. This is reflected in their large error estimates. Near saturation and the very large errors of samples reported by *Marra* [2003] lead us to suspect these ages may be too old.

[26] The  $^{14}\text{C}$  and OSL ages on the silt of unit 3 indicate the age of the unit varies with location, and are younger at higher elevations on the paleoscarp. Two OSL samples were collected from the top and bottom of unit 3 where it overlies unit 2b gravels in the footwall of the thrust (Figures 3 and 6). The sample from base of the silt (NI47), located below the Kawakawa tephra (exposed in this outcrop), yielded an OSL age of  $18.5 \pm 2.4$  ka. Although this age is younger than published  $^{14}\text{C}$  ages of the Kawakawa [*Pillans et al.*, 1993; *Wilson et al.*, 1988], it is consistent with other OSL ages of the unit and inferences based on deposition rates [*Almond et al.*, 2007; *Pillans et al.*, 1993]. Alternatively, it could indicate that the tephra was reworked at this site. One OSL and  $^{14}\text{C}$  sample are collocated at the top of unit 3, and yield identical ages of  $14 \pm 2$  ka (OSL, NI46) and 14.1–14.9 calib kyr B.P. ( $^{14}\text{C}$ , WH05-1), respectively, giving us confidence that the age of the base of the unit is also correct. Sample NI40, from the top of unit 3 (Figure 3) yielded an age of 14.2–15 calib kyr B.P. while samples from higher elevations on the paleoscarp are 11.2–11.6 calib kyr B.P. (NI41, Figure 4) and 9.1–9.5 calib kyr B.P. (NI26, Figures 5 and 6). These dates suggest that the silt of unit 3 and overlying gravels of unit 4 progressively onlapped the scarp over a period of  $>5,000$  years. Two OSL samples were also

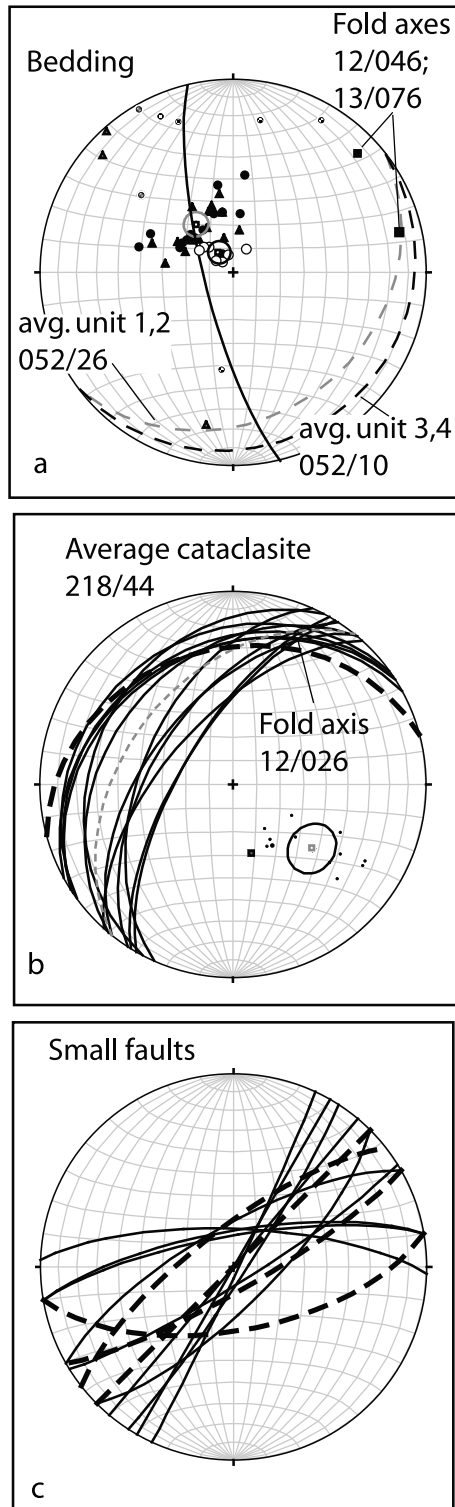


**Figure 9.** Equal-area stereoplots of structures related to Wharekauhau thrust in area shown in Figure 4. (a) Poles to bedding: triangles, unit 1; filled, unit 2; open circles units 3, 4. Fold axis of all unit 1 and 2 data is 13/076, and fold axis 12/046 is small-scale fold in duplex. Average orientation excludes steep beds in duplex and adjacent to thrust (smaller symbols); mean vector and plane are shown by cone of confidence and dashed great circle; gray for units 1 and 2, black for units 3 and 4. (b) Black great circles are cataclasis planes, with poles shown as dots; black dashed line is minor thrust plane (60 cm separation); gray dotted line is mean plane, with mean pole and cone of confidence shown in open square and circle, respectively. Calculated fold axis assumes scatter of planes is due to upward flattening of the thrust. (c) Stereoplot of small-scale faults adjacent to thrust. Solid great circles are normal faults cutting units 1 and 2 at crest of hanging wall anticline, dashed great circles are inferred strike-slip faults that cut up into units 3 and 4.

**Table 1a.** Doserate Contribution of Cosmic Radiation for OSL Samples

Field Sample	Unit	Depth Below Surface (m)	$dD/dt^a$ (Gy/ka)	Easting <sup>b</sup>	Northing <sup>b</sup>	Lab Code
NI42	1	50	$0.0064 \pm 0.0003$	2682480	5979380	WLL577
NI43	2a	45	$0.0078 \pm 0.0004$	2682283	5979577	WLL578
NI46	3	40	$0.0096 \pm 0.0005$	2682077	5980424	WLL579
NI47	3	40	$0.0096 \pm 0.0005$	2682077	5980424	WLL580
NI48	1	50	$0.0064 \pm 0.0003$	2681774	5979712	WLL581
NI49	4? <sup>c</sup>	8	$0.0768 \pm 0.0038$	2683479	5982154	WLL582
NI50	4? <sup>c</sup>	8	$0.0768 \pm 0.0038$	2683469	5982160	WLL583
NI51	marine <sup>c</sup>	25	$0.0204 \pm 0.0010$	2685893	5979228	WLL584
NI52	2b	35	$0.0120 \pm 0.0006$	2682309	5979531	WLL585
NI53	3	3	$0.1376 \pm 0.0069$	2682317	5981050	WLL586
NI54	3	2	$0.1569 \pm 0.0078$	2682302	5981031	WLL587

<sup>a</sup>Contribution of cosmic radiation to the total doserate, calculated as proposed by *Prescott and Hutton* [1994].

<sup>b</sup>Grid reference for NZMS260 sheet R27.

<sup>c</sup>See text for discussion of unit assignments.

collected from anomalously thick unit 3 above 30° SE dipping hanging wall gravels (unit 2b) east of Wharekauhau Stream (Figures 3 and 5). One sample from the middle of the massive silt (NI53) and the other from the base (NI54) yielded ages of  $\sim 18.9 \pm 2.4$  and  $19.5 \pm 3.2$  ka, respectively (Tables 1a and 1b).

[27] Finally, we dated two samples of sandy silts (NI49, NI50) that were collected from stratigraphically high lenses of sand and silt interbedded with fluvial gravels in Papatahi Stream, mapped by *Begg and Mazengarb* [1996] as Waiohine gravels (unit 4). The samples are located only 6–8 m below the top of the stream bluff (i.e., Waiohine surface). These samples yielded ages of  $25.8 \pm 6.8$  (NI49) and  $39.7 \pm 4.4$  (NI50) (Figure 3 and Tables 1a and 1b) that are of uncertain significance. Two interpretations are possible: (1) the fairly thin lenses interbedded with the alluvial gravels may not have experienced sufficient light exposure prior to burial to “zero” the age, resulting in an overestimate of the age of gravels that belong to unit 4, or (2), the gravels may represent a fluvial sequence, not present in Te Mahonge and Wharekauhau streams, that is younger than unit 2 but older than units 3 and 4. This latter interpretation would suggest that the locus of fan deposition shifted to the northeast following the abandonment of the unit 2 fan surface. After the Papatahi fan lobe was deposited, the silt of unit 3 would have then blanketed all the older fan deposits. Later, the unit 4 gravels beneath the Waiohine surface were deposited, with the locus of deposition shifting back toward the southwest. We recognized two extensive silt layers, one above and one below the gravels and sands containing the dated samples (NI49 and NI50), and each characterized by the presence of rooted stumps. The lower silt is 0.5 to 1.5 m thick and apparently continuous from Papatahi Stream to the mouth of the Wharepapa River, while the upper silt is <1 m thick and can be traced intermittently over this same distance. Although the gravels below, between, and above the silts appear similar, we prefer interpretation (2), that the silts bound a fluvial unit of intermediate age between units 2 and 3. Based on the tentative correlation of the silt layers, we estimate that the intervening fluvial unit is  $\sim 6$ –12 m thick and that unit

4 gravels in Wharepapa River and Papatahi streams are no more than a few meters thick (Figure 7).

[28] Our dating results provide important new timing constraints useful for analysis of deformation rates. We note that the ages from unit 3 indicate that the Waiohine gravels (unit 4) were deposited diachronously from  $\sim 15$  ka to <9 ka rather than within a <1–2 kyr interval as inferred by *Grapes and Wellman* [1993] and *Shulmeister et al.* [2000]. In subsequent sections we use the ages summarized on Figure 6 to constrain our interpretations.

#### 4. Geomorphology of the Wharekauhau Fault System

[29] In this section we summarize our geomorphic observations of the entire length of the Wharekauhau fault system. As revealed by the stratigraphic record described above, we interpret the low angle Wharekauhau thrust to be inactive, so we focus this section on which parts of the originally mapped trace of the Wharekauhau thrust [*Begg and Mazengarb*, 1996; *Begg and Johnston*, 2000] show evidence for Holocene slip (especially in 1855) and which appear to be inactive. We show that the active fault system consists of ENE striking strike-slip fault strands and NNE striking folds and blind, or partly inactive, thrusts (Figure 2 and Text S2).

[30] We divided the fault into four segments from north to south: Burlings strike-slip segment, Maunganui thrust segment, Riverslea strike-slip segment, and Wharepapa thrust and strike-slip segment (Figure 2). Details of our observations are provided in Text S2, and are summarized on Figure 2 (inset) and in this section. Faults interpreted as “active” cut the Waiohine surface, as indicated by scarps or displaced/deformed Waiohine gravels; geomorphic evidence of active folding (i.e., blind thrusting) was noted if the Waiohine surface (assumed to be relatively flat) showed broad warping or topographic relief that did not appear to be related to stream downcutting (i.e., younger terrace treads inset into the surface). To document activity in the 1855 earthquake, we noted which scarps were especially steep or fresh looking, (e.g., with a surface slope of  $>25^\circ$ ) by analogy

**Table 1b.** Luminescence Dating Results

Field Sample	Water Content $\delta^a$	U From $^{234}\text{Th}$ ( $\mu\text{g/g}$ )	U From $^{226}\text{Ra}$ , $^{214}\text{Pb}$ , $^{214}\text{Bi}^2$ ( $\mu\text{g/g}$ )	U From $^{210}\text{Pb}$ ( $\mu\text{g/g}$ )	Th From $^{208}\text{Tl}$ , $^{212}\text{Pb}$ , $^{228}\text{Ac}^b$ ( $\mu\text{g/g}$ )	K (%)	$a$ Value	$D_e$ (Gy)	$dD/dt$ (Gy/ka)	OSL Age <sup>c</sup> (ka)
NI42	1.100	1.94 ± 0.22	1.53 ± 0.14	1.78 ± 0.19	6.53 ± 0.10	1.72 ± 0.04	0.101 ± 0.009	222.7 ± 9.8	3.15 ± 0.13	70.7 ± 4.3
NI43	1.352	4.07 ± 0.25	3.63 ± 0.16	4.29 ± 0.23	16.51 ± 0.16	3.04 ± 0.06	0.074 ± 0.022	393.7 ± 70.2	4.81 ± 0.53	81.9 ± 17.2
NI46	1.184	3.33 ± 0.29	3.04 ± 0.19	3.36 ± 0.26	12.42 ± 0.15	2.37 ± 0.05	0.101 ± 0.014	66.0 ± 2.1	4.73 ± 0.32	14.0 ± 1.0
NI47	1.155	2.91 ± 0.33	2.89 ± 0.21	3.00 ± 0.29	11.91 ± 0.17	2.14 ± 0.05	0.081 ± 0.005	80.0 ± 3.0	4.32 ± 0.23	18.5 ± 1.2
NI48	1.277	2.07 ± 0.24	1.98 ± 0.16	1.63 ± 0.21	7.40 ± 0.11	1.92 ± 0.04	0.075 ± 0.009	304.8 ± 24.2	2.87 ± 0.25	106.1 ± 12.4
NI49	1.234	4.31 ± 0.36	4.00 ± 0.23	3.66 ± 0.30	17.29 ± 0.20	3.02 ± 0.06	0.076 ± 0.027	145.6 ± 12.9	5.64 ± 0.56	25.8 ± 3.4
NI50	1.125	4.10 ± 0.28	3.68 ± 0.18	3.70 ± 0.24	16.35 ± 0.18	2.85 ± 0.06	0.083 ± 0.012	185.2 ± 23.2 (SAR) <sup>d</sup>	6.03 ± 0.32	32.9 ± 5.3 (SAR) <sup>d</sup>
NI51	1.124	2.51 ± 0.17	2.17 ± 0.11	2.13 ± 0.15	8.74 ± 0.10	1.84 ± 0.04	0.070 ± 0.023	239.4 ± 4.7	3.46 ± 0.25	39.7 ± 2.2
NI52	1.213	3.81 ± 0.34	3.77 ± 0.22	3.69 ± 0.30	17.02 ± 0.20	3.06 ± 0.06	0.050 ± 0.025 <sup>e</sup>	488.8 ± 23.6	5.24 ± 0.51	141.1 ± 12.3
NI53	1.149	3.20 ± 0.33	2.72 ± 0.21	2.90 ± 0.29	11.74 ± 0.16	2.26 ± 0.05	0.055 ± 0.003	439.9 ± 16.2 (SAR) <sup>d</sup>	4.21 ± 0.22	127.0 ± 10.3 (SAR) <sup>d</sup>
NI54	1.198	3.60 ± 0.36	3.18 ± 0.23	2.60 ± 0.30	13.39 ± 0.18	2.26 ± 0.05	0.067 ± 0.009	378.1 ± 17.7 (SAR) <sup>d</sup>	4.47 ± 0.29	71.0 ± 9.2
								79.5 ± 2.7		72.2 ± 7.8 (SAR) <sup>d</sup>
								87.1 ± 4.0		18.9 ± 1.2
										19.5 ± 1.6

<sup>a</sup>Ratio wet sample to dry sample weight. Errors assumed 50% of  $(\delta - 1)$ .

<sup>b</sup>U and Th content is calculated from the error weighted mean of the isotope equivalent contents.

<sup>c</sup>Age errors are  $1\sigma$ .

<sup>d</sup>These samples were additionally measured by the single aliquot regenerative method (SAR). For these samples, when the two methods agree, ages quoted in the text are the result with the smaller error.

<sup>e</sup>The  $a$  value of this sample was estimated (the  $\alpha$ -irradiated subsample was saturated).

**Table 2.** Radiocarbon Ages From Sandy Silt Unit 3

Sample <sup>a</sup>	NZMS260 Sheet R27 Grid Ref		$\delta^{13}\text{C}^{\text{b}}$ (‰)	Conventional Age <sup>c</sup> (years B.P. $1\sigma$ )	Calibrated Age <sup>d</sup> (95%) (calib years B.P.)	Lab <sup>e</sup>
	Easting	Northing				
WH05-1	2682092	5980398	-28.6	12424 $\pm$ 68	14874–14145	WK18991
NI26	2682247	5980948	-23.9	8387 $\pm$ 82	9520–9090	WK18988
NI40	2682097	5980112	-28.8	12507 $\pm$ 68	14981–14224	WK18989
NI41	2681770	5978628	-25.5	9982 $\pm$ 58	11620–11210	WK18990

<sup>a</sup>All samples are rooted wood from the top of the unit.

<sup>b</sup>The isotopic fractionation ‰ with respect to PDB.

<sup>c</sup>Conventional age as per *Stuiver and Polach* [1977]. Quoted errors are 1 standard deviation due to counting statistics multiplied by an experimentally determined laboratory error multiplier of 1. This is based on the Libby half-life of 5568 years with correction for isotopic fractionation applied.

<sup>d</sup>Calibrated using Calib 5.0.1 (M. Stuiver et al., CALIB 5.0, WWW program and documentation, 2005, available at <http://calib.qub.ac.uk/calib/>). Samples <11,000 years calibrated using Southern Hemisphere calibration [*McCormac et al.*, 2004]; older samples using Intcal04 [*Reimer et al.*, 2004].

<sup>e</sup>Surfaces scraped clean. The wood was washed in ultrasonic bath, then ground. Sample was washed in hot 10% HCl, rinsed and treated with hot 0.5% NaOH. The NaOH insoluble fraction was treated with hot 10% HCl, filtered, rinsed and dried.

with other scarps along the Wairarapa fault zone in similar materials [*Grapes and Downes*, 1997; *Ongley*, 1943; *Rodgers and Little*, 2006; *Schermer et al.*, 2004]. We also documented locations where no scarp is present along the trace mapped by *Begg and Mazengarb* [1996], and where the fault between greywacke and Quaternary gravels is overlapped by Waiohine gravels, and infer that these portions of the thrust have been abandoned since stabilization of the Waiohine surface (12.4–5.4 ka [*Little et al.*, 2009]).

[31] Our geomorphic observations (Text S2) reveal that the most prominent scarps occur along discontinuous, ENE striking faults that trend straight across valleys. These scarps are interpreted as active, steep, strike-slip faults that probably ruptured in 1855. Evidence for dextral slip occurs along the Burlings Segment at Burling Hill, where early Quaternary? gravels are cut by a series of short (<300 m) faults that displace the ridge crest by a total of  $90 \pm 10$  m, and along the Riverslea segment, ~1 km north of Riverslea station, where gullies are offset by  $8 \pm 1$ ,  $8 \pm 2$ , and  $21 \pm 2$  m (Text S2 and Figure 2 inset). Other active strike-slip faults occur as <1 km long, en echelon traces that disrupt the Waiohine surface, e.g., in the Wharepapa segment, where one strand is associated with an ~8 m dextral jog of an incised stream (Figure 3). Recent surface rupture is documented at Riverslea, where trenching shows that a subvertical strike-slip fault has ruptured twice since 897 cal years B.P., with the most recent event being younger than 547 cal years B.P., and interpreted to be the 1855 earthquake (Figure 2 inset and Text S2) [*Little et al.*, 2009].

[32] It is more difficult to demonstrate whether any thrust segments are active, as none that we investigated have distinct scarps that can be clearly associated with a gently NW dipping fault (e.g., “V”-ing across streams and ridges) (Text S2), and there is clear evidence in the Wharepapa segment that Waiohine gravels depositionally overlap the thrust. Quaternary-aged thrusting is indicated by the juxtaposition of greywacke and deformed early? Quaternary gravels along the main strand of the Wharekauhau thrust, and by the apparent uplift of these gravels in the hanging wall of an eastern strand of the thrust along the Riverslea

and Maunganui segments (Figure 2) [*Begg and Mazengarb*, 1996]. However, along the length of the Wharekauhau fault system, thrust traces are buried by Waiohine gravels, and do not exhibit steep scarps on the Waiohine surface, and therefore are considered to be inactive (Figures 2 and 3). Local fresh-looking scarps at the base of steep slopes (e.g., SE of High Maunganui, Figure 2 inset) are reinterpreted as landslide scarps, although it is possible they obscure a throughgoing blind thrust. The principal evidence of Holocene activity along thrust segments occurs at Riverslea, where trenching revealed folding of ~1300 year old gravels along a presumed blind thrust that has an active strike-slip fault in its hanging wall [*Little et al.*, 2009]. Active blind thrusting is also inferred along the Maunganui segment, where a broad low-angle scarp may indicate a fold of the Waiohine surface (Figure 2 inset and Text S2).

[33] The different positions of the inactive Wharekauhau thrust and the active, principally strike-slip, elements of the Wharekauhau fault system suggest that the locus and kinematics of deformation has changed over time. For example, the distinctly more easterly strike, apparently steeper dip, and evidence of dextrally offset surface features along the eastern strand of the fault in the Riverslea segment suggest different kinematics than on the Maunganui segment. The contrast between demonstrably active tectonics at the site near Riverslea Station on the eastern strand, and the lack of evidence of Holocene offset on the western strand suggests that deformation along the Wharekauhau fault system has propagated from northwest to southeast.

## 5. Structural Geology and Slip History of the Wharepapa Segment

### 5.1. Structural Characteristics of the Wharekauhau Thrust

[34] The Wharepapa segment, from Wharepapa River to Palliser Bay, features well exposed outcrops of the Wharekauhau thrust in two locations that have been described by *Grapes and Wellman* [1993]. We focused

our mapping on these outcrops and nearby stratigraphic contacts and geomorphic features in Te Mahonge and Wharekauhau streams (Figures 3, 4, 5, S1, and S2). The basic features of our map do not differ greatly from those of previous workers [Begg and Mazengarb, 1996; Begg and Johnston, 2000; Eade, 1995]; however, our detailed structural and stratigraphic study of the outcrops has led us to different interpretations. Most importantly, we conclude that the Wharekauhau thrust experienced an apparently short-lived and rapid period of slip, and after abandonment, was cut by steeper strike-slip faults. In this section we first describe the thrust and deformation related to the period of thrusting, followed by a description of later strike-slip faulting.

[35] In outcrop, the southern Wharekauhau thrust consists of two subparallel thrust planes that are spaced  $\sim 1$ – $1.5$  m apart. Both thrusts are extremely sharp, marked by a few centimeters of gouge. The higher thrust juxtaposes highly fractured Cretaceous Torlesse greywacke (foliated cataclasite several meters thick, Figure 9b) in its hanging wall to the northwest above steeply dipping unit 1 strata to the southeast. The lower thrust juxtaposes unit 1 above steeply to gently dipping strata of unit 2 (subunits 2b and 2c) (Figures 4, 5, 8, S1, and S2). Between the two fault planes, the slice of steeply dipping strata of unit 1 occurs as a “horse” that is internally folded (Figures 9a, S1, and S2). The structural thickness of unit 1 in this horse (up to  $\sim 100$  m) is  $>10$  times greater than the observed maximum stratigraphic thickness of unit 1 away from the fault (7–9 m). Although the discontinuity of exposure prevents us from verifying the inference, this relationship suggests that unit 1 in the horse is repeated several times by thrust duplexing or distributed deformation (e.g., Figure S1 and S2).

[36] The two thrusts flatten in an eastward direction from northwest dipping to subhorizontal (Figures 4, 5, and 8). Cataclasite fabric in the hanging wall greywacke also flattens upward, from  $68^\circ\text{NW}$  to  $23^\circ\text{NW}$ , with the hinge direction of this antiform trending  $026$  (Figure 9b). No slickenlines were found on the thrust plane. Outcrops in Wharekauhau Stream offer the best constraints on the average orientation of the thrust because subparallel exposures occur on both banks of the stream, although exposure is somewhat obscured by brush on the west bank (Figure 5). A range of strikes from  $210$  to  $225$  ( $\text{N}30$ – $45\text{E}$ ) is permissible from the detailed map relations. However, between Te Mahonge and Wharekauhau streams, the trace of the fault is oriented  $\sim 020$ , and structure contours drawn from data in each stream do not line up, suggesting the two exposures are folded or faulted out of alignment.

[37] The important structural elements displayed by the detailed maps, cross sections and outcrop data (Figures 4, 5, 8, and 9) include the following: In the footwall away from the thrust plane, the (conformable) unit 1–unit 2 contact defines a plane dipping  $2^\circ\text{N}$  (Figure 3). Within  $\sim 100$  m of the thrust, the average dip of bedding in units 1 and 2 is  $\sim 25^\circ\text{SE}$  (Figure 9a). Immediately adjacent to the thrust and in the horse, bedding steepens to subvertical, where the greywacke and units 1, 2a, and the lower part of 2b form a hanging wall anticline and footwall syncline. Near the crest

of the anticline, several steeply SE dipping faults with  $<0.5$  m normal separation cut unit 2, perhaps to accommodate localized extension above the fold crest (Figures 4a, 9c, and S2). The anticline and thrust are overlapped with marked angular discordance by the upper part of unit 2b across a buttress unconformity.

[38] In all locations, strata at the top of unit 2 have a similar dip to those at the bottom of that unit and to beds in unit 1 (Figure 9a). This concordance indicates no measurable tilting during sedimentation of units 1 and 2, although the variability of dips, the sparsity of data near the top of the unit, and the difficulty of measuring bedding in coarse fan gravels could allow for some minor ( $<5^\circ$ ) shallowing up section.

[39] In contrast to the  $24$ – $90^\circ$  (SE) dips of units 1 and 2, units 3 and 4 dips are subhorizontal at Wharekauhau stream and average  $\sim 10^\circ$  at Te Mahonge Stream (Figures 8 and 9a). Much or all of the latter may be a primary dip of those west derived alluvial fan deposits.

## 5.2. Interpretation of Deformation Related to Thrusting

[40] The geometric and stratigraphic relationships suggest initial formation of a fault-propagation fold, followed by the fault tip propagating upward to the surface, and cutting off the steep forelimb. The subvertical dips in the imbricate fault slice of unit 1 and locally in unit 2 immediately below the lower thrust and in units 1 and 2 above the upper thrust (Figures 4, 5, and 8) indicate that the strata were folded prior to thrusting. The eastward shallowing of the thrust planes, and the coincidence of the flat surface with the paleosol within unit 2b (Figure 8) suggests that the faults ramped upward to the contemporary free surface before collapsing (Figure 4b and 5b).

## 5.3. Minimum Displacement on the Wharekauhau Thrust

[41] No slickenlines were observed on the thrust plane, so we assume purely dip-slip displacement to calculate a minimum amount of horizontal shortening required by the cross sections. The cross section in Te Mahonge Stream provides a better estimate of slip magnitude because the hanging wall cutoffs of the contacts between greywacke, unit 1, and unit 2 are exposed on the east side of the stream and the cutoff of the stratigraphic contact between units 1 and 2 within the horse is exposed on the west side of the stream (Figure 4a), so both could be accurately mapped. However, the contacts below the lower thrust are not exposed, so we assume minimum shortening in locating that contact on the cross section (Figure 4b). We further assume that the late stage vertical fault (Figure 4b) does not dramatically change the overall thrust geometry. In cross section A–A' (Figure 4b), which is drawn perpendicular to a thrust strike of  $218$  ( $\text{N}38\text{E}$ ), the amount of horizontal overlap (heave) is  $110$  m on the upper thrust and a minimum of  $140$  m on the lower thrust. The southeastern extent of the imbricate slice is uncertain due to heavy brush, indicated by the dashed line on Figure 4b, but projection of the unit 1–unit 2 contact from the west bank constrains the minimum overlap on the lower thrust. These values do not account for the additional shortening caused by folding of units or thrust

duplexing within the horse. Line length balancing of the unit 1–unit 2 contact by removal of its curvature implies an additional  $\sim 20$  m of fold-related shortening for a total of 280 m. Other cross sections constructed at Te Mahonge stream using thrust strikes varying from N20E to N45E and using the observed range of strikes of contacts and other faults yielded minimum (thrusting + folding) shortening estimates that ranged from 215 to 340 m. On the basis of these calculations we assign a preferred value of  $280 \pm 60$  m to our minimum shortening estimate.

[42] In Wharekauhau Stream, corresponding hanging wall and footwall cutoffs are not exposed so there is less control on total shortening at that site. Cross section B–B' can be used, however, to calculate a minimum heave of  $65 \pm 2$  m on the upper thrust of the horse from the amount of overlap of the greywacke and the fragment of unit 1 in the hanging wall, assuming a thrust strike of N30E (Figure 5b). Doubling that to account for the overlap of unit 1 on the lower fault (and without accounting for any duplexing) gives a minimum of 130 m shortening across both thrusts. Varying the strike of the thrust to account for poor exposure of the surface results in  $<15$  m difference in the heave.

[43] The vertical component of thrusting (throw) is constrained by the elevation difference between the hanging wall and footwall strata, as constrained by our detailed laser mapping. We use the unit 1/unit 2 contact as a marker because the base of unit 1 is not exposed in the footwall. The footwall exposure of the contact is at  $14 \pm 1$  m asl; in the hanging wall, the exposed contact rises to  $96 \pm 1$  m (Figure 3). There, the unit 1/unit 2 contact is eroded and overlapped by unit 4, and the base of the unit 1 gravels extends to an elevation of  $106 \pm 1$  m (Figure 4a). Since unit 1 has a consistent thickness of 7–8 m along this exposure, we can estimate that the unit 1/unit 2 contact originally extended to 112–115 m asl prior to erosion, constraining the throw to 97–102 m. This is a minimum value because the contact is likely folded to lower elevations in the footwall and higher elevations in the hanging wall than the present exposures (Figure 4b).

#### 5.4. Structural and Stratigraphic Constraints on the Timing of Thrust Motion

[44] The structural and stratigraphic relationships lead us to infer that the major period of shortening on the Wharekauhau thrust began at  $\sim 70$  ka. Evidence for the age of initiation of the thrust comes from the observation that beds in units 1 and 2 are parallel to each other at all locations where we could measure them, including adjacent to the thrust (Figure 9a). Although there may have been thrust activity prior to the deposition of unit 1, and/or during the deposition of unit 2b, to cause some (unrecognized) minor fanning of dips within that unit, we infer that deformation of the conformable unit 1–unit 2a contact did not begin until after deposition of the latter. The age of this contact, based on the OSL data described above, is constrained to the interval  $106 \pm 24$  to  $71 \pm 8$  ka. If we are correct in our inference that thrusting began during deposition of the syntectonic unit 2b, then

the OSL data would indicate a thrust initiation age of no older than  $71 \pm 8$  ka.

[45] Stratigraphic and structural evidence further suggest the abandonment of thrusting by  $\sim 20$  ka. Onlap and burial of the paleoscarp by units 3 and 4 and the angular unconformity at the base of unit 3 suggest that the thrust was inactive at this time. The recognition of a buttress unconformity within unit 2b suggests deposition of that unit took place during the waning stages of thrust activity. Above the unconformity, dates on unit 3 nearest the thrust suggest abandonment occurred after  $19.5 \pm 3.2$  (base of unit 3) to 9.1–9.5 ka (top of unit 3) (Figure 6). The sedimentological characteristics of unit 3 (i.e., very fine grained, and of uniform thickness to within  $\sim 20$  m southeast of the thrust) suggest that the thrust was not active during any part of its deposition (i.e., in stark contrast to units 2b, 2c). From these data we infer that the thrust was certainly abandoned by  $\sim 9$  ka, and more likely was abandoned as early as  $\sim 20$  ka.

#### 5.5. Vertical and Horizontal Components of Slip Rate

[46] Our new structural and geochronological data provide estimates of the late Quaternary slip rate of the Wharekauhau thrust. These rates are minima because the amount of heave and throw are minimum values and because the age of the top of unit 2b could be younger than our youngest dated sample. From the range of horizontal shortening estimates at Te Mahonge Stream ( $280 \pm 60$  m) on the unit 1/unit 2 contact, and given the conservative estimate of the duration of thrusting ( $106 \pm 24$  ka to 9.1–9.5 ka), the minimum shortening rate is 1.8–4.7 mm/yr. On the basis of our preferred duration estimate of  $71 \pm 8$  ka to  $19.5 \pm 3.2$  ka, we calculate a minimum rate of 3.5–8.4 mm/yr. The vertical component of slip rate (throw rate) due to the Wharekauhau thrust can also be constrained using the minimum throw of 97–102 m. Using the conservative estimate of thrusting duration, we estimate a minimum vertical throw rate on the Wharekauhau thrust of 0.8–1.4 mm/yr. Using the preferred timing constraints, the minimum throw rate is 1.5–2.5 mm/yr.

#### 5.6. Crosscutting Faults

[47] Structural evidence exists for steeply dipping faults that postdate motion on the Wharekauhau thrust. Although we have not found a continuous, throughgoing fault, several map- and outcrop-scale observations support the hypothesis of late strike-slip faulting that occurs in the vicinity of the inactive thrust traces. The most compelling evidence comes from our detailed mapping. Structure contours drawn parallel to strike from surveyed elevations on the thrust surface indicate that the thrust surfaces in Te Mahonge and Wharekauhau stream are not coplanar, and further show that the outcrop in Te Mahonge Stream has been folded or faulted to lower elevation than that in Wharekauhau Stream. However, since the thrust at both locations shows the same flattening upward geometry (Figures 4b and 5b), and similar strike and dip of the thrust, fault displacement appears more likely than folding.

[48] In outcrop, exposures in Te Mahonge Stream suggest that following erosion of the thrust and deposition of unit 3, several steeply dipping strike-slip(?) faults cut through the Quaternary units (Figures 4 and 9c). Just south of the thrust exposure on the east side of the stream, a fault oriented  $\sim 075/80\text{SE}$  causes  $\sim 3$  m of down to the southeast vertical separation of the contact between units 2 and 3. Cross section relations implied by the fold geometry in unit 2 suggest that the separation on the unit 1–unit 2 contact is up to the southeast (Figure 4b). Because the two contacts are not parallel, the opposite vertical separations can be most simply explained by dextral slip. We also interpret this fault to extend across the stream to the west, where the lower “thrust” has been reoriented to a vertical dip. This fault does not appear to cut up to the Waiohine surface. Several steep faults are also observed cutting hanging wall strata in Te Mahonge stream, but most are too small to show on the map (Figure 4a). These faults are NE striking, steeply dipping faults with at most a few meters of vertical and horizontal separation (Figure 9c). The faults locally cut up into the upper part of unit 4 but do not demonstrably cut the Waiohine surface. The presence of both reverse and normal separations suggests strike-slip faulting; slickenlines were found only on one fault and are subhorizontal.

### 5.7. Deformation of the Waiohine Surface?

[49] Vertically above the exposures of the thrust in Te Mahonge Stream, the Waiohine terrace surface was interpreted by *Grapes and Wellman* [1993] to be warped upward during rupture of the Wharekauhau thrust in 1855 and prior earthquakes. Our new mapping shows that the Waiohine gravels (unit 4), do not show the same dip as the terrace surface, which is mantled by a younger layer of colluvium derived from the hilly topography northwest of the inactive thrust trace. The strata in unit 4 everywhere dip  $<15^\circ$  and onlap depositionally against the more steeply dipping strata in the thrust hanging wall. From these relationships we infer that the Waiohine surface at the top of unit 4 is undeformed and that the local increase in surface slope of the hillside adjacent to the paleoscarp is a primary depositional feature of the landscape and not the result of tectonic deformation.

[50] *Grapes and Wellman* [1993] inferred that  $\sim 20$  m of height difference between the Waiohine surface in the hanging wall and footwall of the thrust at Wharekauhau Stream (Figure 5b) was due to deformation along the thrust. A laser-surveyed topographic profile along the Waiohine surface across the trace of the thrust from NW to SE across the stream shows the surface is 15 m lower on the SE side of the stream, but the dips are low ( $2.5\text{--}5^\circ$ ) and it is not clear if there is a change in dip that can be associated with the trace of the thrust (Figure 5b). We interpret the dips as primary features of the fan surface, which, as described above, appears to have been deposited across the inactive thrust as a steep, locally sourced fan (Figure 7). If the change in slope is indeed due to thrust-related tilting, then the active fault must lie well below the surface, cannot have the same near-surface expression as the (inactive) Wharekauhau thrust, and would have a much slower slip rate ( $<1$  mm/yr as calculated from line balancing of the fan surface in

Figure 5b, assuming it was originally horizontal, and was shortened 4–5 m to obtain its present shape in the last 5–9 kyr).

[51] Deep incision of modern streams below the Waiohine surface, and the contrast between this incision and the depocenters of Lake Onoke and the Ruamahonga River mouth to the east suggests that the Waiohine surface is today being uplifted. Since both the hanging wall and the footwall of the (inactive) Wharekauhau thrust are incised (Figure 3), and since sea level in New Zealand has been relatively stable for the last 6000 years [*Gibb*, 1986], we interpret this incision and uplift to result from uplift in the hanging wall of a blind thrust to the east of the Wharekauhau thrust and near the western margin of the Wairarapa valley  $\sim 4$  km to the east (Figure 2). Because the Waiohine surface is not preserved east of Wharepapa River, and because the surface was not originally flat, but part of a SE dipping alluvial fan system, it is difficult to document this incision more precisely, or to narrow the location of the inferred active thrust. Active subsidence of the Wairarapa valley near the Ruamahonga River during the Holocene has been inferred from drill hole data (K. Wilson, personal communication, 2008), a relationship that supports our inference of a west-side up fault farther to the west. Seismic reflection data [*Barnes and Audru*, 1999] also suggest that a blind thrust fault may be present in the offshore region to the south of the western margin of the Wairarapa valley (see below). The Battery Hill fault is east-side up and thus cannot be responsible for northwest-side up uplift, but the Pounui anticline may play a role in the active deformation (Figure 2) [*Begg and Mazengarb*, 1996].

### 5.8. Uplift of Footwall Relative to Sea Level

[52] An interesting pattern is shown by the elevations of the unit 1/unit 2 contact in a footwall transect parallel to the coast. As described above, this contact is inferred to have formed as a subhorizontal contact near sea level in an estuarine lagoon. Relative to present-day mean sea level, this contact rises from west to east from  $<14 \pm 1$  m at Wharekauhau Stream (in the west) to  $25 \pm 4$  m at Wharepapa River, indicating an average apparent dip of  $2\text{--}6^\circ$  to the west and suggesting the presence of a broad fold in the footwall of the Wharekauhau thrust to the west of Lake Onoke (Figure 3). Furthermore, since the elevation of sea level at  $\sim 80$  ka was similar to present [*Gibb*, 1986], the contact has been uplifted 14–25 m in that time frame, an eastwardly increasing uplift rate relative to mean sea level of 0.08–0.3 mm/yr. We do not know if this deformation is related to the Pounui anticline or to another structure such as the aforementioned blind thrust.

### 5.9. Deformation in the 1855 Earthquake

[53] *Grapes and Wellman* [1988], following *Lyell* [1868], assumed the Wharekauhau thrust ruptured in 1855 at Te Mahonge Stream, and this has been passed down through the literature [e.g., *Begg and Mazengarb*, 1996; *Grapes and Downes*, 1997; *Little and Begg*, 2005; *Rodgers and Little*, 2006; *Sibson*, 2006]. A review of the historical record as part of this study [*Downes and Grapes*, 1999; *Ongley*, 1943;

E. R. Schermer, unpublished data, 2006] indicates that there was no definitive contemporary account of 1855 surface rupture at the coast at Te Mahonge or Wharekauhau streams, and as we have demonstrated above, the gently dipping Wharekauhau thrust at those locations has not slipped in >9 ka. Uplifted beach ridges at Turakirae Head, and an abrupt eastward limit to the coastal uplift recorded in 1855 by surveyor *Roberts* [1855] were previously attributed to thrust movement on the Wharekauhau thrust [*Darby and Beanland*, 1992]. Reanalysis of the pattern of 1855 uplift led [*Beavan and Darby*, 2005; *McSaveney et al.*, 2006] to conclude that the fault that was responsible for the very high magnitude (up to 6.4 m) but short wavelength of uplift at Turakirae Head must have been a local thrust east of the head. *McSaveney et al.* [2006] suggest that a left step in the Wairarapa fault, possibly at the Mukamuka Stream shear zone of *Begg and Mazengarb* [1996], was responsible for the uplift of Turakirae Head in repeated “characteristic” earthquakes. Severe landsliding in the Rimutaka Range during the 1855 earthquake [*Grapes and Downes*, 1997] may have obscured the trace of the surface rupture near the coast. We conclude that 1855 (and prior) uplift at Turakirae Head was produced by slip on a fault, of uncertain exact location, near Mukamuka Stream. We refer to this fault as the Mukamuka fault in subsequent discussion. Surface rupture in 1855 is also inferred to have occurred on discontinuous steep, strike-slip faults along the southeast front of Wharekauhau Mountain, near Riverslea, and at Burling Hill (Figures 2 and 3). It is possible that the strike-slip segments were linked at depth by blind thrusts that caused uplift and landsliding on Wharekauhau Mountain and High Mauganui Hill, but we cannot confirm the existence of these blind thrusts or fault slip on them during 1855.

## 6. Offshore Continuation of Faults

[54] Detailed bathymetric mapping and seismic reflection profiling [*Barnes and Audru*, 1999; *Barnes*, 2005; *Barnes et al.*, 2008] suggest that two NE striking active faults offshore of Palliser Bay may be related to the onland part of the greater Wairarapa fault zone (Figure 1). Both faults are discontinuous and ~30–35 km long, and neither shows evidence for dextral offset of bathymetric features at resolution of the mapping (~10 m [*Barnes*, 2005]). The Nicholson Bank fault (Figure 1) is approximately aligned with Turakirae Head and may connect to a fault that runs up the Orongorongo Valley; however, although this strand is prominent in the offshore bathymetry, workers onshore [e.g., *Begg and Mazengarb*, 1996] have not recognized an active fault in that valley. A second offshore strand (called the “offshore Wharekauhau thrust” by [*Barnes et al.*, 2008]) strikes NE along the western wall of Wairarapa canyon where it bounds the western margin of the Quaternary Wairarapa basin (Figures 1 and 2). A bathymetric fault scarp along this feature, together with an abundance of large landslides nearby, led *Barnes* [2005] to suggest that this strand may have ruptured in 1855. Seismic reflection data (line A of *Barnes and Audru* [1999]) shows a fault with

~2.0–2.3 km of vertical reverse separation. Corrected for apparent dip, the fault dips 60°–65°NW. Although *Barnes and Audru* [1999] infer that this strand connects to the Wharekauhau thrust in Te Mahonge Stream, the shallow shelf region has not been surveyed, so it is permissible, and we suggest more likely, that the fault instead runs onshore near Mukamuka Stream (as shown in Figure 2), where it could have been associated with the uplift of Turakirae Head in 1855. The seismic line also shows a shallow NW dipping thrust splay to the southeast of the main strand, intersecting the main fault at 1.2s TWT (~1.5 km depth below the seafloor) which may connect to the (inactive, low-angle) Wharekauhau thrust, as it projects to the coast at the approximate location of the outcrops in Te Mahonge Stream. The reflection profile also shows some normal and reverse separation faults farther east that do not cut upward through Pleistocene units [*Barnes and Audru*, 1999], including possible candidates for the blind reverse fault that has led to uplift of the Wharekauhau thrust footwall. The reverse faults have small offset (~200 m vertical throw on the subbasin basement contact), and appear to die upward into folds, although the shallow part of the record is not definitive.

## 7. Synthesis of Quaternary Deformation, Sedimentation, and Geomorphology of the Southern Wairarapa Region

[55] Combining our new data with previous work onshore and offshore yields an improved picture of the tectonic evolution of the southern Wairarapa region. Offshore seismic data suggest that prior to formation of the wave-cut surface at the base of unit 1, a 2–3 km thick sedimentary basin (the Wairarapa basin) filled with late Cenozoic strata [*Barnes and Audru*, 1999; *McClymont*, 2000; *Rollo*, 1992]. Marine terraces cut at sea level highstands over the last ~450 ka appear to be differentially uplifted and folded around the Rimutaka anticline [*Begg and Mazengarb*, 1996; *Ota et al.*, 1981], suggesting that a thrust to the east of the anticline (e.g., the Mukamuka fault) had been active for several hundred thousand years prior to the deposition of unit 1, so is possible that the Mukamuka fault was the original basin-bounding structure near the Palliser Bay coast. Near the end of the last interglacial (~70–80 ka), our data suggest initiation of the Wharekauhau thrust in its present location northwest of the depocenter of unit 2, possibly as a splay of the original basin-bounding fault. Throughout the time span of deposition of unit 2b, sedimentation appears to have outpaced tectonism, as there is no noticeable growth folding in this unit.

[56] A major period of folding and faulting on the Wharekauhau thrust occurred between the deposition of unit 2b and unit 3, in the interval from ~70–20 ka. Deformation apparently continued after the end of unit 2b deposition, as all of unit 2 is tilted adjacent to the thrust. Following thrusting, streams incised across the thrust and, locally, parallel to the scarp. More than 45 m of erosional relief was created on the unit 2b surface during this time (Figure 4b and 5b). By ~20 ka, the basal part of unit 3 had

begun to mantle this eroded, postthrusting landscape. Between  $\sim 15$ – $9$  ka, the top of unit 3 overlapped northwestward across the trace of the inactive Wharekauhau thrust. The  $>5000$  year period of landscape stability represented by unit 3 and by the lack of dip fanning in the overlying gravels of unit 4 suggests a prolonged period of thrust inactivity. Stream channels eroded through the thrust were later completely or partially filled in again with fluvial gravel (unit 4) during the time period from  $\sim 15$  ka to  $<9$  ka. A zone of steep, strike-slip faults crosscut the abandoned thrust and Waiohine surface; some faults cut the base of unit 4 but not the top, suggesting their initiation before  $\sim 9$  ka. Incision of the Waiohine surface between the Wharekauhau thrust and Lake Onoke, and back-tilting of the unit 1–2 contact suggest that after the death of the Wharekauhau thrust, a younger blind thrust may have propagated eastward to the current western margin of the southern Wairarapa Valley. Connected to the main Wairarapa fault, the Mukamuka fault has apparently remained active, or been reactivated in the Holocene, uplifting Turakirae Head and the Rimutaka anticline in five great earthquakes since 7 ka, including 1855 [McSaveney *et al.*, 2006].

[57] Along the length of the Wharekauhau fault system, the principal evidence of Holocene slip is on ENE striking discontinuous strike-slip faults (Text S2). The most recent surface rupture (1855) on the Wharekauhau fault system appears to have been on these strike-slip fault strands, with displacement much less than on the Wairarapa fault. Thrust motion in 1855, if any, resulted in subtle folding at the surface without surface rupture.

## 8. Discussion and Conclusions: Distribution of Contractional Strain in the Southern Wairarapa Region and Implications for Convergent Margin Tectonics

[58] Our results, which suggest a short period of rapid (3.5–8.4 mm/yr) shortening on the Wharekauhau thrust from  $\sim 70$  to 20 ka, followed by its abandonment, and replacement by a complex set of strike-slip and blind thrusts at the south coast after  $\sim 20$  ka, have important implications for our understanding of how strain is distributed in the upper plate of the subduction zone at obliquely convergent margins. In this section we consider the role of the Wharekauhau fault system in partitioning plate boundary deformation over time.

[59] Nicol *et al.* [2007], using fault slip data, geological cross sections, seismic reflection data, and paleomagnetic data, calculated total shortening and shortening rates (averaged over the last  $\sim 5$  Ma) on several transects across the Hikurangi margin. They argue that, for a transect just north of our study area, since  $\sim 5$  Ma, the component of plate convergence transferred to the upper plate is only  $\sim 10\%$  of the total and decreases farther to the north, where the margin is presumably less strongly “coupled.” Nicol and Wallace [2007] also found that the shortening rate across the southern Wairarapa region, averaged over the last  $\sim 1.5$  Myr, as determined by geological data ( $3.3 \pm 3.6$  mm/yr), compares favorably with that determined by

GPS data over the last 10–15 years ( $3.9 \pm 1.8$  mm/yr), and infer that  $\sim 85\%$  of the margin-normal plate motion is accommodated by slip on the plate interface (e.g., in megathrust earthquakes). If our preferred estimate of shortening along the Wharekauhau thrust is correct, at a minimum of 3.5 mm/yr, then for a short period of time ( $\sim 50$  kyr), the Wharekauhau thrust took up virtually all of the component of shortening transferred to the Australian plate, and a significant portion (11–30%) of the margin-normal plate convergence rate of 30 mm/yr. Furthermore, the abandonment of the Wharekauhau thrust suggests that its share of the deformation budget was transferred elsewhere, either onto other upper plate faults, or onto the plate interface, i.e., implying an unsteady linkage between faults.

[60] The rate of shortening on the Wharekauhau thrust, during its period of activity, exceeds that of all other faults in New Zealand, with the exception of the Alpine fault (at 5–10 mm/yr [Norris and Cooper, 2001]), suggesting that this fault, for a time, played an extremely important role in accommodating plate motion. For a single fault to accommodate such a (temporarily) high contraction rate suggests that the Wharekauhau thrust may have been kinematically linked (at times) to the subduction megathrust, as suggested by Rodgers and Little [2006] and Little *et al.* [2009] for the Wairarapa fault. Nicol and Wallace [2007] argue that on a regional scale (i.e., across the width of the upper plate), the fraction of plate motion that is accommodated in the upper plate ( $\sim 15\%$ ) versus on the plate interface ( $\sim 85\%$ ) has been roughly constant over the last 1.5 Myr. Our data, however, suggest that on a smaller spatial and temporal scale, significant variations in fault slip rate and migration of the locus of deformation in the upper plate have occurred. If the Wharekauhau thrust accommodated a significant portion of plate convergence for  $\sim 50$  kyr, were the fraction of interface slip, the magnitude of megathrust earthquakes, or recurrence interval of slip on the plate interface different than they are today?

[61] In a recent paleoseismic study of the Wairarapa fault, Little *et al.* [2009] established a record of five earthquakes in the last  $\sim 5000$  years on the central section of the Wairarapa fault (including 1855); the most recent two events also ruptured the Wharekauhau fault near Riverslea Station. This trench-derived paleoseismic record does not agree in detail with that obtained from uplifted beach ridges at Turakirae Head, where McSaveney *et al.* [2006] documented three “great” earthquakes in the same period of time. Little *et al.* [2009] suggest that the mismatch between these two records may be explained by variable interaction of the Wairarapa fault zone with the subduction megathrust, or by variation in the style and location of surface faulting at the southern end of the greater Wairarapa fault zone. In the first scenario, the largest earthquakes corupture the Wairarapa fault and the plate interface, causing substantial uplift of the coastal platform at Turakirae Head. Smaller events, however, may only rupture the upper plate faults (e.g., Wairarapa and Wharekauhau), and cause little or no uplift at the coast. The second scenario suggests that variable uplift at the coast is related to the complexity of faulting in the southernmost part of the Wairarapa fault zone. In events such as 1855, the

Wairarapa fault would connect to the Mukamuka fault, causing large uplift at Turakirae Head, which allows preservation of a stranded beach ridge. In other events, rupture at the coast is taken up by other faults farther to the east, causing less uplift, and thus less preservation potential, of a beach ridge at Turakirae Head. This scenario is most consistent with our data, which imply that some Wairarapa fault events corupture the Wharekauhau fault system, while others may cause surface folding farther east near Lake Onoke. Any event in which the Wairarapa fault is linked with faults east of the Mukamuka fault could result in the “omission” of a beach ridge from the paleoseismic record at Turakirae Head.

[62] We infer that present-day deformation (including during 1855) at the southern end of the Wairarapa Fault zone is partitioned between slip on (1) the more western Wairarapa-Mukamuka fault system (dominantly dextral slip but also causing local uplift of the coast near Turakirae

Head; (2) a series of discontinuously expressed, near-vertical strike-slip faults and linking blind oblique-reverse thrusts near the trace of the older (inactive) Wharekauhau thrust; and (3) a possible blind thrust fault between Lake Onoke and the western margin of the Wairarapa Valley. The spatial and temporal complexity of the Wharekauhau fault system and the importance it has had in accommodating upper plate deformation argue for an unsteady linkage between upper plate faults and between these faults and the plate interface.

[63] **Acknowledgments.** We thank Dave Walsh of Wharekauhau Station, Charlie Matthews of Waiorongomai Station, and Hugh Saywell of Riverslea Station for access. Dene Carroll, Brad Ilg, and Mike Henry helped with field work. This project was funded by the “It’s our fault” program of GNS Science, and a Western Washington University sabbatical leave to E.R.S. We also thank Mark Quigley and an anonymous reviewer for helpful comments on the manuscript.

## References

- Adamiec, G., and M. J. Aitken (1998), Dose-rate conversion factors: Update, *Ancient TL*, 16, 37–50.
- Almond, P. C., F. L. Shanhuna, U. Rieser, and J. Shulmeister (2007), An OSL, radiocarbon and tephra isochron-based chronology for Birdlings Flat loess at Ahuriri Quarry, Banks Peninsula, Canterbury, New Zealand, *Quat. Geochronol.*, 2, 4–8, doi:10.1016/j.quageo.2006.06.002.
- Barnes, P. M. (2005), The southern end of the Wairarapa fault, and surrounding structures in Cook Strait, in *The 1855 Wairarapa Earthquake symposium—Proceedings Volume*, edited by R. Langridge, J. Townend, and A. Jones, pp. 66–71, Greater Wellington Reg. Council, Wellington, New Zealand.
- Barnes, P. M., and J.-C. Audru (1999), Quaternary faulting in the offshore Flaxbourne and Wairarapa Basins, southern Cook Strait, New Zealand, *N. Z. J. Geol. Geophys.*, 42, 349–367.
- Barnes, P. M., and B. Mercier de Lépinay (1997), Rates and mechanics of rapid frontal accretion along the very obliquely convergent southern Hikurangi margin, New Zealand, *J. Geophys. Res.*, 102, 24,931–24,952, doi:10.1029/97JB01384.
- Barnes, P. M., B. Mercier de Lépinay, J.-Y. Collot, J. Delteil, and J.-C. Audru (1998), Strain partitioning in the transition area between oblique subduction and continental collision, Hikurangi margin, New Zealand, *Tectonics*, 17, 534–557, doi:10.1029/98TC00974.
- Barnes, P. M., N. Pondard, G. Lamarche, J. Mountjoy, R. Van Dissen, and N. J. Litchfield (2008), It’s Our Fault: Active Faults and Earthquake Sources in Cook Strait, *Client Rep. WLG2008-56*, 43 pp., Natl. Inst. of Water and Atmos. Res., Auckland.
- Beanland, S. (1995), The North Island Dextral Fault Belt, Hikurangi subduction margin, New Zealand, Ph.D. thesis, 323 pp., Victoria Univ. of Wellington, Wellington, New Zealand.
- Beanland, S., and J. Haines (1998), A kinematic model of active deformation in the North Island, New Zealand, determined from geological strain rates, *N. Z. J. Geol. Geophys.*, 41(4), 311–324.
- Beavan, J., and D. Darby (2005), Fault slip in the 1855 Wairarapa earthquake based on new and reassessed vertical motion observations: Did slip occur on the subduction interface?, in *The 1855 Wairarapa Earthquake Symposium—Proceedings Volume*, edited by R. Langridge, J. Townend, and A. Jones, pp. 31–41, Greater Wellington Reg. Council, Wellington, New Zealand.
- Beavan, J., P. Tregoning, M. Bevis, T. Kato, and C. Meertens (2002), Motion and rigidity of the Pacific Plate and implications for plate boundary deformation, *J. Geophys. Res.*, 107(B10), 2261, doi:10.1029/2001JB000282.
- Begg, J. G., and M. R. Johnston (2000), Geology of the Wellington area, New Zealand, *Geol. Map 64*, Inst. of Geol. and Nucl. Sci., Ltd., Lower Hutt, New Zealand.
- Begg, J. G., and C. Mazengarb (1996), Geology of the Wellington area, *Geol. Map 22*, Inst. of Geol. and Nucl. Sci., Ltd., Lower Hutt, New Zealand.
- Collen, J. D., and P. Vella (1984), Hautotara, Te Muna and Ahiruhé formations, Middle to Late Pleistocene, Wairarapa, New Zealand, *J. R. Soc. N. Z.*, 14(4), 297–317.
- Darby, D. J., and S. Beanland (1992), Possible source models for the 1855 Wairarapa earthquake, New Zealand, *J. Geophys. Res.*, 97, 12,375–12,389, doi:10.1029/92JB00567.
- Darby, D., and J. Beaven (2001), Evidence from GPS measurements for contemporary interplate coupling on the southern Hikurangi subduction thrust and for partitioning of strain in the upper plate, *J. Geophys. Res.*, 106, 30,881–30,892, doi:10.1029/2000JB000023.
- DeMets, C., R. G. Gordon, D. F. Argus, and S. Stein (1990), Current plate motions, *Geophys. J. Int.*, 101, 425–478, doi:10.1111/j.1365-246X.1990.tb06579.x.
- DeMets, C., R. G. Gordon, D. F. Argus, and S. Stein (1994), Effects of recent revisions to the geomagnetic reversal time scale on estimates of current plate motion, *Geophys. Res. Lett.*, 21, 2191–2194, doi:10.1029/94GL02118.
- Downes, G., and R. H. Grapes (1999), The 1855 Wairarapa, Earthquake, New Zealand—Historical data, *Sci. Rep. 99/16*, 267 pp., Inst. of Geol. and Nucl. Sci., Ltd., Lower Hutt, New Zealand.
- Eade, R. E. (1995), Late Quaternary geology of the Wharekauhau area, Ocean Beach, Palliser Bay, B.Sc. Honors thesis, 50 pp., Victoria Univ. of Wellington, Wellington, New Zealand.
- Fitch, T. J. (1972), Plate convergence, transcurrent faults, and internal deformation adjacent to southeast Asia and the western Pacific, *J. Geophys. Res.*, 77, 4432–4461, doi:10.1029/JB077i023p04432.
- Formento-Trigilio, M. L., D. W. Burbank, A. Nicol, J. Shulmeister, and U. Rieser (2003), River response to an active fold and thrust belt in a convergent margin setting, North Island, New Zealand, *Geomorphology*, 49, 125–152, doi:10.1016/S0169-555X(02)00167-8.
- Ghani, M. A. (1978), Late Cenozoic vertical crustal movements in the southern North Island, New Zealand, *N. Z. J. Geol. Geophys.*, 21, 117–125.
- Gibb, J. G. (1986), A New Zealand regional Holocene sea-level curve and its application to determination of vertical tectonic movements, *R. Soc. N. Z. Bull.*, 24, 377–395.
- Grapes, R., and G. Downes (1997), The 1855 Wairarapa, New Zealand, earthquake—Analysis of historical data, *Bull. N. Z. Natl. Soc. Earthquake Eng.*, 40(4), 271–368.
- Grapes, R., and H. Wellman (1988), The Wairarapa fault, report, Res. Sch. of Earth Sci., Victoria Univ. of Wellington, Wellington, N. Z.
- Grapes, R. H., and H. W. Wellman (1993), Wharekauhau Thrust (Palliser Bay) and Wairarapa Fault (Pigeon Bush), *Geol. Soc. New Zealand Misc. Publ.*, 79B, 27–44.
- Kelsey, H. M., S. M. Cashman, S. Beanland, and K. R. Berryman (1995), Structural evolution along the inner forearc of the obliquely convergent Hikurangi margin, New Zealand, *Tectonics*, 14(1), 1–18, doi:10.1029/94TC01506.
- Lang, A., and G. A. Wagner (1997), Infrared stimulated luminescence dating of Holocene colluvial sediments using the 410 nm emission, *Quat. Sci. Rev.*, 16, 393–396, doi:10.1016/S0277-3791(96)00106-0.
- Lee, J. M., and J. G. Begg (2002), Geology of the Wairarapa area, scale 1:250,000, *Geol. Map 211*, 251 sheets, 266 p., Inst. of Geol. and Nuclear Sci., Ltd., Lower Hutt, New Zealand.
- Lensen, G., and P. Vella (1971), The Waiohine River faulted terrace sequence: Recent crustal movements, *R. Soc. N. Z. Bull.*, 9, 117–119.
- Little, T. A., and J. G. Begg (2005), All-day field trip to the Wairarapa fault and 1855 rupture sites, in *1855 Wairarapa Earthquake Sesquicentennial Symposium Volume*, pp. 1–28, Greater Wellington Reg. Council, Wellington, New Zealand.
- Little, T. A., R. Wightman, R. J. Holcombe, and M. Hill (2007), Transpression models and ductile deformation of the lower crust of the Pacific Plate in the central Southern Alps, a perspective from structural geology, in *A Continental Plate Boundary: Tectonics at South Island, New Zealand*, *Geophys. Monogr. Ser.*, vol. 175, edited by D. Okaya, T. Stern, and F. Davey, pp. 271–288, AGU, Washington, D. C.
- Little, T. A., E. R. Schermer, R. Van Dissen, J. Begg, and R. Carne (2008), Southern Wairarapa Fault and Wharekauhau Thrust (Palliser Bay): Field trip 5, *Geol. Soc. N. Z. Misc. Publ.*, 124B, 75–120.
- Little, T. A., R. Van Dissen, E. R. Schermer, and R. Carne (2009), Late Holocene surface ruptures on the southern Wairarapa fault, New Zealand: Link between earthquakes and the raising of beach ridges on a rocky coast, *Lithosphere*, 1, 4–28, doi:10.1130/L7.1.
- Lyell, C. (1856), Sur les effets du tremblement de terre du 23 Janvier, 1855 à la Nouvelle Zélande, *Bull. Geol. Soc. Fr.*, Ser. 2, 13, 661–667.

- Lyell, C. (1868), *Principals of Geology or the Modern Changes of the Earth and Its Inhabitants*, 10th ed., John Murray, London.
- Marra, M. J. (2003), Last interglacial beetle fauna from New Zealand, *Quat. Res.*, *59*, 122–131, doi:10.1016/S0033-5894(02)00022-4.
- McCaffrey, R. (1992), Oblique plate convergence, slip vectors, and forearc deformation, *J. Geophys. Res.*, *97*, 8905–8915, doi:10.1029/92JB00483.
- McClymont, A. F. (2000), A gravity survey of the Wharekauhau Thrust, Palliser Bay, New Zealand, *N. Z. J. Geol. Geophys.*, *43*, 303–306.
- McCormac, F. G., A. G. Hogg, P. G. Blackwell, C. E. Buck, T. F. G. Higham, and P. J. Reimer (2004), SHCal04 Southern Hemisphere calibration 0–11.0 cal kyr BP, *Radiocarbon*, *46*, 1087–1092.
- McSaveney, M. J., I. J. Graham, J. G. Begg, A. G. Beu, A. G. Hull, K. Kim, and A. Zondervan (2006), Late Holocene uplift of beach ridges at Turakirae Head, south Wellington coast, New Zealand, *N. Z. J. Geol. Geophys.*, *49*, 337–358.
- Mouslopoulou, V., A. Nicol, T. A. Little, and J. Walsh (2007), Displacement transfer between intersecting regional strike-slip and extensional fault systems, *J. Struct. Geol.*, *29*, 100–116, doi:10.1016/j.jsg.2006.08.002.
- Nicol, A., and L. M. Wallace (2007), Temporal stability of deformation rates: Comparison of geological and geodetic observations, Hikurangi subduction margin, New Zealand, *Earth Planet. Sci. Lett.*, *258*, 397–413, doi:10.1016/j.epsl.2007.03.039.
- Nicol, A., R. Van Dissen, P. Vella, B. Alloway, and A. Melhuish (2002), Growth of contractional structures during the last 10 m.y. at the southern end of the Hikurangi forearc basin, New Zealand, *N. Z. J. Geol. Geophys.*, *45*, 365–385.
- Nicol, A., C. Mazengarb, F. Chanier, G. Rait, C. Uruski, and L. Wallace (2007), Tectonic evolution of the active Hikurangi subduction margin, New Zealand, since the Oligocene, *Tectonics*, *26*, TC4002, doi:10.1029/2006TC002090.
- Norris, R. J., and A. F. Cooper (1995), Origin of small scale segmentation and transpressional thrusting along the Alpine Fault, New Zealand, *Geol. Soc. Am. Bull.*, *107*(2), 231–240, doi:10.1130/0016-7606(1995)107<0231:OOSSSA>2.3.CO;2.
- Norris, R. J., and A. F. Cooper (2001), Late Quaternary slip rates and slip partitioning on the Alpine Fault, New Zealand, *J. Struct. Geol.*, *23*, 507–520, doi:10.1016/S0191-8141(00)00122-X.
- Ongley, M. (1943), Surface trace of the 1855 earthquake, *Trans. R. Soc. N. Z.*, *73*, 84–89.
- Ota, Y., D. N. Williams, and K. R. Berryman (1981), Parts sheets Q27,R27 and R28-Wellington, 1st ed., Dep. of Sci. and Ind. Res., Wellington, New Zealand.
- Pillans, B., M. McGlone, A. Palmer, D. Mildenhall, B. Alloway, and G. Berger (1993), The last glacial maximum in central and southern North Island, New Zealand: A paleo-environmental reconstruction using the Kawakawa tephra Formation as a chronostratigraphic marker, *Palaeogeogr. Palaeoclimatol. Palaeoecol.*, *101*, 283–304, doi:10.1016/0031-0182(93)90020-J.
- Prescott, J. R., and J. T. Hutton (1994), Cosmic ray contributions to dose rates for luminescence and ESR dating: Large depths and long-term variations, *Radiat. Meas.*, *23*, 497–500, doi:10.1016/1350-4487(94)90086-8.
- Reimer, P. J., et al. (2004), IntCal04 terrestrial radiocarbon age calibration, 26–0 ka BP, *Radiocarbon*, *46*, 1029–1058.
- Reyners, M. (1998), Plate coupling and the hazard of large subduction thrust earthquakes at the Hikurangi subduction zone, New Zealand, *N. Z. J. Geol. Geophys.*, *41*(4), 343–354.
- Roberts, E. (1855), Memorandum on the earthquake in the islands of New Zealand, January 23, 1855, in *Te Ika a Maui, or New Zealand and Its Inhabitants*, edited by R. G. Taylor, p. 471, Wertem and MacIntosh, London.
- Rodgers, D., and T. A. Little (2006), World's largest coseismic strike-slip offset: The 1855 rupture of the Wairarapa Fault, New Zealand, and implications for displacement/length scaling of continental earthquakes, *J. Geophys. Res.*, *111*, B12408, doi:10.1029/2005JB004065.
- Rollo, J. (1992), Geophysical investigations of the southwestern Wairarapa region of New Zealand, M.Sc. thesis, Victoria Univ. of Wellington, Wellington, New Zealand.
- Schermer, E. R., R. Van Dissen, K. R. Berryman, H. M. Kelsey, and S. M. Cashman (2004), Active faults, paleoseismology and historical fault rupture in the northern Wairarapa, North Island, New Zealand, *N. Z. J. Geol. Geophys.*, *47*, 101–122.
- Shulmeister, J., P. Barrett, and M. Marra (2000), Modern and ancient sedimentary environments of the southern Wairarapa, *Geol. Soc. N. Z. Misc. Publ.*, *108B*, 1–15.
- Sibson, R. H. (2006), Charles Lyell and the 1855 Wairarapa earthquake in New Zealand: Recognition of fault rupture accompanying an earthquake, *Seismol. Res. Lett.*, *77*(3), 358–363, doi:10.1785/gssrl.77.3.358.
- Stuiver, M., and H. A. Polach (1977), Discussion: Reporting of <sup>14</sup>C data, *Radiocarbon*, *19*, 355–363.
- Stuiver, M., and P. J. Reimer (1993), Extended <sup>14</sup>C database and revised CALIB radiocarbon calibration program, *Radiocarbon*, *35*, 215–230.
- Teyssier, C., B. Tikoff, and M. Markley (1995), Oblique plate motion and continental tectonics, *Geology*, *23*(5), 447–450, doi:10.1130/0091-7613(1995)023<0447:OPMACT>2.3.CO;2.
- Van Dissen, R. J., and K. R. Berryman (1996), Surface rupture earthquakes over the last 1000 years in the Wellington region, New Zealand, and implications for ground shaking hazard, *J. Geophys. Res.*, *101*, 5999–6019, doi:10.1029/95JB02391.
- Walcott, R. I. (1984), The kinematics of the plate boundary zone through New Zealand: A comparison of short- and long-term deformations, *Geophys. J. R. Astron. Soc.*, *79*, 613–633.
- Wallace, L. M., J. Beavan, R. McCaffrey, and D. Darby (2004), Subduction zone coupling and tectonic block rotations in the North Island, New Zealand, *J. Geophys. Res.*, *109*, B12406, doi:10.1029/2004JB003241.
- Wallace, L. M., J. Beavan, R. McCaffrey, K. R. Berryman, and P. Denys (2007), Balancing the plate motion budget in the South Island, New Zealand using GPS, geological and seismological data, *Geophys. J. Int.*, *168*, 332–352, doi:10.1111/j.1365-246X.2006.03183.x.
- Wang, N. (2001), Optically stimulated luminescence dating techniques and their application to dating the loess in southern North Island, M.Sc. thesis, 131 pp., Victoria Univ. of Wellington, Wellington.
- Wilson, C. J. N., V. R. Switsur, and A. P. Ward (1988), A new <sup>14</sup>C age for the Oruanui (Wairakei) eruption, New Zealand, *Geol. Mag.*, *125*, 297–300, doi:10.1017/S0016756800010232.

T. A. Little and U. Rieser, School of Geography, Environment and Earth Sciences, Victoria University of Wellington, PO Box 600, Wellington, New Zealand.

E. R. Schermer, Geology Department, Western Washington University, MS 9080, Bellingham, WA 98225, USA. (schermer@geol.wvu.edu)